Summary of major revisions: (1) The manuscript was rewritten following the reviewers' suggestions. all the symbols used are consistent. Four figures were removed and about 1800 words were removed from main text of the revised manuscript. (2) The manuscript has been edited by two senior English editors from Nature Springer Language editing services.

Response to Reviewer # 1

1. General Comments

This is an important paper with interesting Figures on the regional variation of surface temperature trends over China, and their relation to regional precipitation and SSR. The biggest challenge for this reviewer is that I unsure exactly what the elegant Figures show. There are critical gaps between the methods section and the Figures. The legends rather than the text try to explain the content of the Figures, and they are written for the authors, not for a global audience, which will struggle to follow the missing steps in the logic. The reader cannot connect the symbols in Methods to the symbols in the Figures, and the description of the Figures.

Reply: Thank you for the high recommendation and constructive comments. We have carefully checked and revised logical structure of paper and unified the symbols for Methods and Figures. As a result, four figures were removed and about 1800 words were removed from main text of the revised manuscript. Below please find our point to point response to your comments.

2. Technical details

Comments: Methods uses T_{raw} and $T_{adjusted}$ and monthly anomalies, as well as '*z*' for a regression fit to monthly anomalies of *T*. Do all the graphs show anomalies? Which ones show $T_{adjusted}$? Which ones show regression fits '*z*'?

Reply: In this study, all of trends and regression analyses are based on the monthly anomalies of temperatures (*T*, including $T_{s\text{-}max}$, $T_{s\text{-}min}$, $T_{a\text{-}max}$, $T_{a\text{-}min}$), surface solar radiation (R_s) and precipitation (P) during 1960-2003. We explicitly claimed in Lines 222-223: "The linear trends reported in this study were calculated via linear regression based on the monthly anomalies of T, R_s, and P" and in Lines 239-240: "The effect of Rs/P on Ts-max/Ta-max was determined via a multiple linear regression (Roy and Haigh, 2011) of the monthly anomalies using the following equation:".

In this revised paper, we deleted the Eqs. (1) and (3) and revised Eq. (2) into:

$$T = S_{Rs} \cdot R_s + S_P \cdot P + c + \varepsilon$$

All the confusing symbols including T_{raw}, $T_{adjusted}$, and 'z' were removed from the revised paper. After revision, the main manuscript and figure captions are consistent. We further revised the figure captions to make them clearer and more concise.

Comments: Eq (1), 2 and 5 are just textbook definitions, which are poorly defined for this specific analysis. They use 'a' and 'b' as symbols for different coefficients in 1, 2 and 5. The values for these (a, b) in this analysis may appear in later figures, but the reader has to guess how they were actually computed. Which Figures show which coefficients or adjusted variables is unclear, because they are largely labeled the same: e. g Ts-max or Ta-min, or just 'PC'.

Reply: In this revised paper, we deleted the Eqs. (1) and (3) and revised Eq. (2) (see our response to your last comment). The symbols of 'a', 'b', and 'PC' were removed from the revised paper. Following comments from the other reviewers, the figures of partial correlation coefficients were moved from main text to the supplementary material section with full names labelled.

Comments: Relabel PCa, PCb, PCc, PCd etc with a clear connection to a numbered equation coefficient. Use the same specific language to describe the coefficient in both methods and text introducing the Figure.

Reply: See our response to your last comment. We have removed the symbols of 'PC' and relabeled partial correlation coefficients with full names.

Comments: Consider adding a simple label to distinguish $T_{adjusted}$ from T in the Figures.

Reply: In the revised paper, we used 'Adjusted temperatures' (e.g. 'Adjusted $T_{s\text{-}max}$') instead of $T_{adjusted}$ (see Figs 7, Figs 8, Figs 9d and Figs S10 in new version).

Comments: L177-180 Comment that the number of sunshine duration stations (105 in Wang et al. 2015a) is still small compared with the T_a data. How well are they distributed in western China?

Reply: Wang et al. (2015a) only used the sunshine duration data where direct observations of surface solar radiation are available to make comparison. Sunshine duration and T_a have been observed at each weather station and their numbers are the same for T_a and sunshine duration. In this study, we used the recently released daily meteorological data at ~2000 stations, which is the best data one can obtained now. Its spatial distribution was shown in Figure 1.

Comments: L242 What are the coefficients 'a' and 'b'; and their uncertainties? Cross-reference where you show these. When you reach Figs 5 and 6, it is unclear how they relate to Eq (2)

Reply: We revised the equation (see also our response to your comment No. 1). After revision, the main text and figure captions are consistent in the symbols. We have added the 95% confidence intervals to S_{Rs} and S_P based on two tailed t-test, e.g. in lines 342-345: "As shown in Fig S7 shows, $T_{s\text{-}max}$ was the most sensitive to R_s, followed by $T_{a\text{-}max}$, and the national means for $T_{s\text{-}max}$ was 0.092±0.018 °C (W m^{-2})$^{-1}$ (95% confidence level) and $T_{a\text{-}max}$ was 0.035±0.010 °C (W m^{-2})$^{-1}$ (95% confidence level)." and Lines 379-381: "The national mean sensitivities of $T_{s\text{-}max}$ and $T_{a\text{-}max}$ to P were −0.321±0.098 °C 10 mm^{-1} and −0.064±0.054 °C 10 mm^{-1} (95% confidence level), respectively.".

Comments: L245 There are no equations 3 and 4.

Reply: The equation 5 is the third equation in original manuscript. In this revised paper, we deleted the Eqs. (1) and (3), and one equation was kept.

Comments: L251 and Figs 2 and 3. Are these T_{raw} or $T_{adjusted}$?

Reply: Both Fig 2 and Fig 3 are yearly anomalies of original data of temperatures without adjusting impacts of R_s and P. Only Fig. 7, 8, 9d, and S10 were adjusted temperature and they were explicitly claimed in the figure captions.

Comments: Section 3.1.1 and Table 1, all these results are presented as mean trends with no estimate of uncertainty. Add some error estimates.

Reply: We have added the 95% confidence intervals for all of trends in new version.

Comments: Section 3.2.1 You need an explicit explanation of Fig 5 and then 6, The reader cannot see clearly how they were constructed. What are these partial correlation coefficients using precipitation as control? Do they relate to the $T_{adjusted}$ in (5) or the sensitivities in (2)? Nothing has been defined or connected logically (and Eq (3) and (4) are missing? Same issues for Figure 8 and 9.

Reply: We have added an explicit explanation of partial correlation coefficients and the logical connection between partial correlation analysis and multilinear regression analysis in Methods: "The coefficients of determination (R^2) for the multilinear regression equation (Eq (1)) are shown in Fig S3, and they indicate the portion of the variance of T that could be attributed to that of R_s and P. High coefficients of determination were obtained, which showed that the linear regression performed well, particularly for South China and the North China Plain. To separate the contributions of R_s and P, we further calculated the partial correlation coefficients between R_s and T (or P and T), which are shown in Fig S4 and Fig S5." (Lines 244-250).

In addition, we have added explicit introduction in the caption of Figs 5 (Figs S4 in new version): "The linear partial correlation coefficients calculated based on the monthly anomalies of R_s and T after avoiding the effect of precipitation (P), which indicates the proportion of variances of T that are attributed to the variation of R_s.".

We have added similar introduction in the caption of Figs 8 (Figs S5 in new version).

Comments: Fig 6 Is this the coefficient ‘a’ in Eq (2)? Where do you show coefficient ‘b’? Is it in Fig9?

Reply: Figs 6 (Figs S7 in new version) show the coefficient ‘a’ (‘S_{R_s}’ in new version) and Figs 9 (Figs S9 in new version) show the coefficient ‘b’ (‘S_P’ in new version). We have replaced ‘a’ with ‘S_{R_s}’ and ‘b’ with ‘S_P’ and used the same symbols in Methods and Figures.

Comments: Fig 11 Is this the first time $T_{adjusted}$ is plotted?

Reply: Yes, it is. We have added the label(‘adjusted’) in all Figures of adjusted temperatures (see Fig 7, Fig 8, Fig 9 and Fig S10 in new version), e.g. ‘Adjusted $T_{s\text{-}max}$’ in Fig 7.

Comments: L136 and L770 cite different references for the dataset.

Reply: We make it consistent and cited Cao et al.

3. Language issues

The structuring of sentences is generally very good, but verbs and tenses need occasional editing, but I will leave this to later editing. An example is 106 LST… plays an important role in climate change 107 research because it directly relates to the land surface energy budget. Previously, Ts 108 values used in regional climate research were primarily derived.

Reply: We have carefully checked English usage of this, and tried to make it more concise and clearer. As a result, more than 1400 words was reduced. The manuscript has been edited by two senior English editors from Nature Springer Language editing services.

Response to Reviewer # 2

1. General Comment:

This paper analyzed the spatial patterns of Ts and Ta and their relations with SSR and precipitation using the observations. It is important to study the mechanism of T changes in the warming climate in regional scales. I think this article is publishable after major corrections.

Reply: Thanks for your highly recommendation and the insightful comments, which substantially improve the paper. Below please find our point to point response to your comments.

2. Major

Comment: Eq (1) is not needed, "linear trend" or “Linear regression” should be enough.

Reply: We have replaced the Eq (1) to a statement in Lines 222-223 that “The linear trends reported in this study were calculated via linear regression based on the monthly anomalies of T, R_s, and P. ”.

Comment: Please discuss why the $T_{adjusted}$ is calculated? State its actual meaning and applications.

Reply: Thanks for your positive comments. We have added the description in Lines 251-256: “To determine the effect of R_s/P on the analyzed temperatures, we removed their effects from their original time series of $T_{s\text{-}max}$ and $T_{a\text{-}max}$ based on the multilinear relationship calculated in Eq (1). Then, we calculated the trends from both the original and adjusted time series. By comparing the derived trends of the original and adjusted time series, we quantitatively assessed the effect of R_s/P on $T_{s\text{-}max}$ and $T_{a\text{-}max}$, particularly for the spatiotemporal pattern of their trends.”.

Comment: The detailed descriptions are not necessary in Figure captions and can be moved to the text.

Reply: Following the reviewer’s suggestion, we substantially reduced the figure captions.

3. Minor

Comment: Line 54: Hegerl and Zwiers is missing in the references

Reply: We have added this literature to references. (Lines 537)

Comment: Is that 1990?

Reply: Yes, it is 1990. We have changed the 1900 to 1990.

Comment: Please check $T_{s\text{-}max}$ and $T_{a\text{-}max}$ trends. By eye, both values should be close.

Reply: We have checked the results of $T_{s\text{-}max}$ and $T_{a\text{-}max}$ trends. The results in paper is right.

Comment: Line 277-281: Mechanism of the difference should be mentioned here.

Reply: We have added the mechanism analysis of those difference as followed in main text. "Although previous studies have indicated that the microclimate (e.g. urban heat island) has a larger effect on minimum temperatures because of the lower and more stable boundary layer at night (Zhou and Ren, 2011; Christy et al., 2009), many investigators argue that variability in R_s is the primary reason for the daily contrast in warming rates (Sanchez-Lorenzo and Wild, 2012; Makowski et al., 2009)." (Lines 288-292).

Comment: Line 284: greater than

Reply: Corrected as suggested.

Comment: Line 294: Significant difference. Can you clarify how significant it is please?

Reply: We deleted this sentence from the revised paper. In the revised paper, 95% confidence intervals were added to all the trends.

Comment: Line 374: along the coast

Reply: Corrected as suggested.

Comment: Line 534: References

Reply: Corrected as suggested.

Comment: Line 570: Eastling et al and Line. 638: Ohmura; They are not referenced in the text, please check.

Reply: Both references were cited in the main text. 'Eastling et al' is cited in Lines 285-288: "The warming rate of $T_{s\text{-}min}$ ($T_{a\text{-}min}$) was significantly faster than that of $T_{s\text{-}max}$ ($T_{a\text{-}max}$) and the warming rates of all temperatures in the cold seasons were substantially greater than those in the warm seasons (Li et al., 2015; Liu et al., 2004; Easterling et al., 1997).". 'Ohmura et al' is cited in Lines 351-354: "Our rate of decrease was considerably less than the global average diminishing rate (form approximately −2.3 to −5.1 W m^{-2} $10yr^{-1}$) between the 1960s and the 1990s (Gilgen et al., 1998; Liepert, 2002; Stanhill and Cohen, 2001; Ohmura, 2006)"

Comment: Ta-min in Figs 5,6,8,9 can be removed, since they don't give much information. They can be briefly discussed in the text.

Reply: Corrected as suggested. We have moved the Figs 5, 6, 8, 9 to the supplementary material and their discussion in main text was substantially reduced.

Contributions of Surface Solar Radiation and Precipitation to the Spatiotemporal Patterns of Surface and Air Temperature Warming in China from 1960 to 2003

Jizeng Du[1,2], Kaicun Wang[1,2*], Jiankai Wang[3], Qian Ma[1,2]

[1]College of Global Change and Earth System Science, Beijing Normal University, Beijing, 100875, China

[2]Joint Center for Global Change Studies, Beijing 100875, China

[3]Chinese Meteorological Administration, Beijing, 100081, China

Corresponding ~~Author~~author: Kaicun Wang, College of Global Change and Earth System Science, Beijing Normal University. Email: kcwang@bnu.edu.cn; Tel: +086 10-58803143; Fax: +086 10-58800059.

Submitted to Atmospheric Chemistry and Physics

~~November~~ February 1~~6~~8, ~~2016~~2017

Abstract

Although ~~the~~ global warming has been ~~successfully~~ attributed to ~~the~~ ~~elevated~~increases in atmospheric greenhouses gases, the ~~reasons for~~mechanisms underlying spatiotemporal patterns ~~the~~ of warming ~~rates~~ trends ~~are still~~remain under debate. ~~In this paper~~Herein, we ~~report~~ analyszed surface and air warming ~~based on~~ observations recorded ~~collected~~ at 1,977 stations in China from 1960 to 2003. Our results showed ~~that~~ a significant spatial pattern for the warming of the daily maximum surface (T_{s-max}) and air (T_{a-max}) temperatures ~~showed a significant spatial pattern~~, and the pattern was stronger in ~~the~~ northwest China and weaker in South China and the North China Plain. These warming spatial patterns ~~are~~ were attributed to surface shortwave solar radiation (R_s~~SSR~~) and precipitation (P), which represent the key parameters of the surface energy budget. During the study period, R_s~~SSR~~ decreased by −1.50±0.42 W m^{-2} 10yr^{-1} in China, ~~and~~ which caused the trends ~~of~~ in T_{s-max} and T_{a-max} to decrease~~d~~ by 0.139 and 0.053 °C 10yr^{-1}, respectively. More importantly, the decreasing rates in South China and the North China Plain ~~had an extremely~~were much higher ~~dimming rates~~ than those in other regions. The spatial contrasts ~~of~~ in the trends of T_{s-max} and T_{a-max} in China ~~are~~ were significantly reduced after adjusting for the ~~impact~~ effect of R_s and P~~SSR and precipitation~~. For example, after adjusting for the effect of R_s and P, the difference

带格式的 ...

in ~~warming rates~~the T_{s-max} and T_{a-max} values between the North China Plain and the Loess Plateau was reduced by 97.8% and 68.3%~~ for Ts-max and Ta-max~~, respectively~~.~~ , ~~After adjusting for the impact of SSR and precipitation,~~ the seasonal contrast ~~of~~ in T_{s-max} and T_{a-max} decreased by 45.0% and 17.2%, respectively, and the daily contrast ~~of~~ in the warming rates of the surface and air temperature decreased by 33.0% and 29.1%~~ over China~~, respectively. This study ~~shows~~ showed that the ~~an essential role of~~ land energy budget ~~in determining~~plays an essential role in the identification of regional warming patterns.

1. Introduction

~~With the rapid development of~~Increases in observational data and ~~the~~ rapid developments in simulation ~~abilities~~ capacity of climate models have provided evidence for the phenomenon of ~~,~~ global warming ~~has been regarded as undeniable~~ (Hartmann et al., 2013), and~~.~~ t~~T~~he increases in anthropogenic greenhouse gases and other anthropogenic ~~impacts~~ effects are ~~believed to be~~considered the primary causes~~ of global warming~~. However, ~~there are~~ significant spatial and temporal heterogeneities in climate warming have been observed~~,~~. ~~i.e.~~For example, faster warming rates occur in semiarid regions and a “warming hole” has been identified in the central United States (Boyles and Raman, 2003; Huang et al., 2012). These spatiotemporal heterogeneities ~~, which~~

带格式的: 字体: 加粗
带格式的: 字体: 加粗
带格式的: 字体: 加粗
带格式的: 字体: 加粗
带格式的: 字体: 加粗
带格式的: 字体: 加粗
带格式的: 字体: 加粗
带格式的: 字体: 加粗
带格式的: 字体: 加粗, 倾斜
带格式的: 字体: 加粗
带格式的: 字体: 加粗, 倾斜
带格式的: 字体: 加粗
带格式的: 字体: 加粗
带格式的: 字体: 加粗
带格式的: 字体: 加粗
带格式的: 字体: 加粗
带格式的: 字体: 加粗
带格式的: 字体: 加粗
带格式的: 字体: 加粗

represent~~s~~ a major barrier to the reliable detection and attribution of global warming (Tebaldi et al., 2005; Mahlstein and Knutti, 2010). Furthermore, ~~the~~ uncertainties in model simulations generally increase from ~~the~~ global to ~~the~~ regional scales because of uncertainty in regional climatic responses to global change (Hingray et al., 2007; Mariotti et al., 2011). Therefore, ~~it is crucial to research not only~~investigations of the spatial and temporal patterns of regional climate changes ~~but also~~and regional climatic response mechanisms to global change are crucial for increasing the accuracy of models designed to detect and explain the causes of~~. This approach can improve confidence in the detection and attribution of~~ global climate change and predictions of future regional climate change.

The spatial heterogeneity of climate warming can be attributed to local climate factors and anthropogenic factors (Karl et al., 1991). For the ~~former~~local climate factors, ~~local~~ determining factors such as cloud ~~amounts~~ cover and precipitation (P) can significantly influence the speed of regional warming ~~speeds~~ (Hegerl and Zwiers, 2007; Lauritsen and Rogers, 2012). ~~Those s~~Spatial heterogeneities in climate-factor trends ~~make important contributions to~~ have an important influence on various changes in the land-surface energy balance. ~~Existing s~~Studies have ~~indicated~~ demonstrated that an increase in cloud cover~~s~~ can diminishes the surface solar radiation (R_s)~~downward shortwave solar radiation to the land surface, thus~~and therefore ~~reducing~~ reduces the

带格式的: 字体: 倾斜

daytime temperature (Dai et al., 1997; Zhou et al., 2010; Taylor et al., 2011), although it has the potential to increase night-time ~~while potentially increasing nighttime~~ temperature~~s~~ by intercepting outgoing longwave radiation (Shen et al., 2014; Campbell and VonderHaar, 1997).

Precipitation (*P*) can alter the proportion of surface absorbed energy partitioned into sensible heat flux ~~and~~ and latent heat flux~~,~~; therefore ~~and therefore~~it has an inevitable ~~impact~~ effect on both land-surface and near-surface air temperatures (Wang and Dickinson, 2012; Wang and Zhou, 2015). ~~In addition~~Additionally, ~~*precipitation*~~ *P* ~~plays~~ has a ~~key role~~significant effect ~~in~~ on ~~the~~ soil thermal inertia and the response of surface vegetation, ~~causing~~ which results in an important feedback ~~to~~ for regional and global warming (Wang and Dickinson, 2012; Seneviratne et al., 2010; Ait-Mesbah et al., 2015; Shen et al., 2015).

带格式的: 字体: 倾斜

In addition to local climate factors, regional climate systems are significantly affected by the anthropogenic emissions of aerosols ~~have a significant effect on the regional climate system~~. Studies have indicated that ~~improving~~ improvements in air quality in recent decades ~~has led to brightening~~ over North America and Europe have led to brightening effect (Wild, 2012; Vautard et al., 2009), whereas ~~surface shortwave solar radiation (SSR) has declined in~~ East Asia and India ~~with increasing air~~

~~pollution~~have led to declines in R_s (Xia, 2010; Menon et al., 2002; Wang et al., 2012; Wang et al., 2015a). Consequently, ~~the~~ variations in ~~SSR~~Rs may have an ~~impact~~ effect on both local and global climate change (Wild et al., 2007; Wang and Dickinson, 2013b).

Changes in l~~L~~and cover ~~change~~ can also alter the energy exchange between the land surface and the atmosphere~~;~~, ~~moreover, it has~~ and such changes have the potential to ~~impact~~ affect regional climates (Falge et al., 2005; Bounoua et al., 1999; Zhou et al., 2004). Previous studies have suggested that urbanization and other land-use changes contribute to promoting the warming effect caused by greenhouse gases (Kalnay and Cai, 2003; Lim et al., 2005; Chen et al., 2015). Overall, the ~~impacts~~ effects of these factors on climate change may be very important ~~on~~ at the regional scale~~, leading~~ and could lead to ~~a~~ marked spatial differences in regional climate change~~,~~; ~~whereas~~ however, they are usually omitted from the detection and attribution of climate change ~~on~~ at the global scale (Karoly and Stott, 2006).

China ~~has~~ is a vast territory ~~and abundant types~~that has an abundance of climactic zones stretching from tropical to cold temperate, ~~with~~ and a special alpine climate is observed over the Tibet Plateau. ~~In addition~~Additionally, the dramatic economic development and explosive population growth in China in recent decades ~~has~~ have caused significant changes in land cover ~~change~~ and ~~serious~~ sever air pollution,

带格式的: 字体: 倾斜

带格式的: 字体: 倾斜, 下标

including frequent haze events (Yin et al., 2016; Cheng et al., 2014; Wang et al., 2016). The climatic diversity and intensive human activity in this region will likely lead to a unique response to global warming with obvious spatial differences in climate change.

Karl et al. (1991) ~~had~~ analyzed the observational records for the period 1951-1989 and~~,~~ ~~finding~~ found that ~~China's temperature~~ warming trends in China were faster than those of the United States but slower than those of the former Soviet Union. Several studies ~~had~~ have revealed that the warming rate in Northwest China ~~had been~~was approximately 0.33-0.39 °C 10yr^{-1} during the second half of the last century (Li et al., 2012; Zhang et al., 2010), which was significantly higher than the average warming rate over China ~~(~~of 0.25 °C 10yr^{-1}~~)~~ (Ren et al., 2005) or ~~that on a global scale~~the average global rate of ~~(~~0.13 °C 10yr^{-1}~~)~~ (Hegerl and Zwiers, 2007). The ~~Air~~ air temperatures~~s~~ (T_a) over the Tibet Plateau ~~have~~ has increased by 0.44 °C 10yr^{-1} over the last 30 years (Duan and Xiao, 2015), ~~which was~~and this rate is considerably faster than the overall warming rate in the Northern Hemisphere (0.23 °C 10yr^{-1}) and worldwide (0.16 °C 10yr^{-1}) (Hartmann et al., 2013). To provide insights on global warming and improve the accuracy of future climate change predictions, u~~U~~nderstanding the characteristics and mechanisms of regional climate change is critical~~ to advancing the knowledge and predication of future climate change~~.

带格式的: 字体: 倾斜

带格式的: 字体: 倾斜, 下标

T_a is a common metric for ~~judging~~ determining climate change on the global or regional scales. ~~However, I~~The land surface temperature (T_s) is ~~beginning to play an increasingly~~also important ~~role~~ in climate change research because of ~~it has the distinct advantage of being~~ its direct~~ly~~ ~~related~~ relationship ~~to~~ with the land surface energy budget. Previously, T_s values used in regional climate research are primarily derived from satellite retrievals or reanalysis datasets (Weng et al., 2004; Peng et al., 2014), ~~both of~~ which both have ~~good~~ satisfactory global coverage but questionable accuracy and integrity. Furthermore, satellite-derived T_s values are only available under clear sky conditions, thus limiting their ~~application~~ applicability ~~to~~ in climate change studies.

In China, both T_s and T_a ~~has been~~are measured as ~~a~~ conventional meteorological observation ~~item~~ parameters by nearly all weather stations~~, as is T_a~~. An analysis of the spatiotemporal patterns of these parameters identified a close relationship between T_s and T_a, which indicates that T_s and T_a present equivalent accuracy when used to determine ~~This study found that observations of T_s have a good relationship with T_a in terms of spatial-temporal patterns and can equally accurately reflect~~ the characteristics of climate change. More importantly, T_s is more sensitive than T_a to the local land surface energy budget~~, particularly surface solar radiation (SSR) and precipitation~~.

~~From the perspective of energy, b~~Both R_s and P ~~SSR and precipitation~~ are key

带格式的: 字体: 倾斜

带格式的: 字体: 倾斜, 下标

带格式的: 字体: 倾斜

带格式的: 字体: 倾斜, 下标

带格式的: 字体: 倾斜

带格式的: 字体: 倾斜

带格式的: 字体: 倾斜

带格式的: 字体: 倾斜

factors controlling the land surface energy budget; therefore, ~~their~~ changes in these two factors most likely cause regional differences in the warming rate of T_a (Wild, 2012; Manara et al., 2015; Hartmann et al., 1986). ~~For the first time~~To our knowledge, this study ~~analyzed~~ presents the first analysis of the relationship between R_s (and P) and T_a/T_s ~~between SSR (and precipitation) and T_a or T_s in terms of~~based on their spati~~al-~~otemporal patterns and we further quantified the ~~impact~~ effect of ~~the~~ variations of R_s and P on T_a/T_s~~SSR and precipitation on T_a and T_s~~ in China for the period ~~of~~ 1960–2003.

This ~~paper~~ article is organized as follows~~:~~. Section 2 introduces the data and methods used in the study. Section 3 ~~includes three parts: the first part~~ describes the spatial and temporal patterns of climate warming over China,~~; the second part analyzes~~ analyses the ~~impact~~ effect of the variation in R_s and P on T_a/T_s,~~SSR and precipitation on T_a and T_s;~~ and ~~the third part illustrates~~examines the spatial and temporal patterns of the warming trend of T_a/T_s~~T_a and T_s~~ after adjusting for the ~~impact~~ effects of R_s and P~~SSR and precipitation.~~, which eliminated the~~The adjustment removed impact~~effects of R_s and P ~~land-atmosphere~~on warming ~~interaction on the warming, leaving impact of~~and highlighted the effects of large-scale warming caused by ~~the~~ elevated concentrations of atmospheric greenhouse gases~~substantially~~. Moreover,~~Our results show that adjustment substantially reduced~~ the spatial contrast ~~of~~in the warming trends

带格式的: 字体: 倾斜

带格式的: 字体: 倾斜, 下标

带格式的: 字体: (默认) Times New Roman

of T_a/T_s~~Ta and Ts~~ in China was substantially reduced after adjusting for the effect of R_s and P~~,~~, and this result is consistent with the expectations under global warming. Finally, Section 4 presents a summary and discussion. ~~which is agree with the expectation of global warming. A summary and discussion are presented in Section 4.~~

2. Data and methods

2.1. Data

The meteorological observational data used in this study are included recently released daily meteorological datasets, ~~including~~ such as the China National Stations' Fundamental Elements Datasets V3.0 (CNSFED V3.0), ~~which can be~~and they were downloaded from ~~the~~ China's National Meteorological Information ~~Center~~ Centre (http://data.cma.gov.cn/data) (Cao et al., 2016). ~~This~~ These datasets ~~includes~~ included observations of T_s, T_a, ~~the~~ barometric pressure, relative humidity, and sunshine duration. All of the observational records of the climate variables ~~include~~ were subjected to quality control measures, and ~~homogenization of~~ the ~~processes of~~ data acquisition and compilation.

As shown in Figure 1, ~~shows that~~ the number of stations used in this study (1,977 ~~selected~~ stations selected from a total of 2,479 stations) ~~is abundant and~~ was

带格式的: 字体: 倾斜

带格式的: 字体: 倾斜

significantly ~~greater~~ higher than ~~in~~ that of previous studies (i.e., 57-852 stations) ~~(Kukla and Karl, 1993; Shen and Varis, 2001; Liu et al., 2004; Li et al., 2015);~~ (Kukla and Karl, 1993; Shen and Varis, 2001; Liu et al., 2004; Li et al., 2015). ~~therefore~~Therefore, the observational data ~~have~~ provided better spatial coverage and higher confidence ~~of~~ in the detection of ~~detecting~~ regional climate change than in previous studies (Fig. 1). Our study is the first to use ~~the observations of~~ T_s observation as a parameter for identifying ~~for research into~~ regional climate change.

带格式的: 字体: 倾斜

Observations of T_s ~~at~~ from weather stations are different from T_s data retrieved via other approaches, such as satellite ~~data~~images and reanalysis. ~~All of the observational fields of T_s are~~The T_s observations were performed in 4 ~~m~~ × 2 m square bare land plots proximal to the ~~in a~~ weather stations. The surface of the observational fields ~~must be kept~~was loose, grassless, ~~,~~ and flat, and at the same level as the ground surface of the weather station. Three thermometers, ~~are placed on the surface of the observational field,~~ including a surface thermometer, a surface maximum thermometer, and a surface minimum thermometer were placed ~~. The thermometers are deposited on the surface of the observational field~~ horizontal to the surface of the observational field, with~~ly:~~ half of each thermometer ~~is~~ embedded in the soil and the other half ~~is~~ exposed to the air. When the observational field ~~is~~ was covered by snow, the thermometers ~~are~~ were ~~removed from the snow and~~ placed on the snow surface. ~~In addition~~Additionally, the

带格式的: 字体: 倾斜

exposed parts of the thermometers ~~must be~~ were ~~kept~~ cleaned ~~clean~~ to remove ~~from~~ dust and dew.

~~To~~ We verif~~y~~ied the reliability of the T_s observational records by analyzing~~, we analyzed the~~ the relationship between T_a and T_s ~~in the observed records for~~ during 1960~~–~~-2003. As shown in Figure~~s~~ S1, the mean Pearson Correlation Coefficients between daily maximum land surface temperature ($T_{s\text{-}max}$~~-~~) and daily maximum air temperature ($T_{a\text{-}max}$~~-~~) calculated from the monthly anomalies were 0.775, 0.843, and 0.806 for the annual, warm, and cold seasonal scales, respectively, and these values were statistically significant (99% confidence level) for all stations. The mean correlation coefficients between the daily minimum land surface temperature ($T_{s\text{-}min}$) and daily minimum air temperature ($T_{a\text{-}min}$) ~~$T_{s\text{-}min}$ and $T_{a\text{-}min}$~~ were 0.861, 0.842, and 0.865 for the annual, warm, and cold seasonal scales, respectively, and these values were statistically significant (99% confidence level) for all stations. The ~~high~~ high correlations indicated ~~between T_a and T_s indicates~~ that ~~the~~ observations of either T_s or T_a could be used for ~~are reliable for detecting~~ climate change detection.

~~SSR is t~~The most fundamental energy resource for T_s and T_a ~~.~~is R_s. In m~~M~~ost previous studies, ~~had used~~ the observed R_s have been used~~SSR~~ to analyze the relation~~ship~~ between the variation in R_s ~~SSR~~ and T_a over ~~Mainland~~ China. However,

带格式的: 字体: 倾斜
带格式的: 字体: 倾斜
带格式的: 字体: 倾斜
带格式的: 字体: 倾斜
带格式的: 字体: 倾斜
带格式的: 字体: 倾斜
带格式的: 字体: 倾斜
带格式的: 字体: 倾斜
带格式的: 字体: 倾斜, 下标
带格式的: 字体: 倾斜
带格式的: 字体: 倾斜
带格式的: 字体: 倾斜
带格式的: 字体: 倾斜, 下标
带格式的: 字体: 倾斜

fewer sites were used for R_s ~~SSR~~ observations than ~~were far less numerous than those~~ for other climatic variables~~, i.e.~~; for example, only 85 sites were used for R_s ~~SSR~~ observations in Liu et al. (2004) and only~~;~~ 90 sites were used in Li et al. (2015).

~~More i~~Importantly, ~~it was found that~~ sensitivity drift~~ing~~ ~~of~~ the instruments used for the R_s ~~SSR~~ observations led to a faster dimming rate before 1990, and ~~that~~ instrument replacements from 1990 to 1993 ~~had~~ resulted in a false~~ly~~ sharp increase in ~~SSR~~ R_s (Wang, 2014; Wang et al., 2015a). The ~~sparse~~ limited distribution and low quality of ~~SSR~~ R_s observations ~~make it difficult to quantify the variation in SSR and detect its impact on climate change~~ have impeded the wide scientific application of this parameter.

~~We t~~Therefore, we used sunshine duration-derived ~~SSR~~ R_s ~~in this study~~, which is based on an effective hybrid model developed by Yang et al. (2006). This model has subsequently been improved (Wang et al., 2015a; Wang, 2014) and it has ~~proved to be~~ performed well in regional and global applications (Tang et al., 2011; Wang et al., 2012). Sunshine duration-derived ~~*solar radiation*~~ R_s not only ~~can~~ accurately reflects the ~~impact~~ effects of clouds and aerosols on the ~~SSR~~ R_s but also ~~can~~ more exactly reveals long-term ~~SSR~~ trends (Wang et al., 2015a; Wang, 2014). Additionally, ~~Sunshine~~ sunshine duration-derived R_s values are ~~has a~~ better ~~correlation~~ correlated with the satellite retrievals ~~-derived SSR~~, ~~reanalysis~~reanalyzes, and climate model simulations ~~of SSR~~ than ~~the observed SSR~~ R_s values observed ~~in China~~from observation (Wang et al.,

带格式的: 下标

带格式的: 字体: 倾斜

带格式的: 字体: 倾斜, 下标

带格式的: 下标

带格式的: 下标

2015a).

The data are collected by a total of~~re are~~ 2,474 meteorological stations ~~reporting data~~; however, the lengths of the effective observation records for the stations are different. ~~In addition~~Additionally, only a small number of stations were installed before ~~existed prior to~~ 1960, and the observational records of T_s at many stations ~~became significantly abnormal~~ were anomalous after 2003 because of automation. Therefore, in our analysis, we selected 1,977 meteorological stations (see Fig~~.~~ 1) ~~that~~ for which the ~~valid data of~~ observation records with valid data were ~~must be~~ longer than 30 years during the ~~period of~~ 43 years between 1960 and 2003.

The monthly ~~anomaly~~ anomalies relative to the 1961-1990 climatology ~~was~~ were calculated based on a monthly mean value of the daily ~~observation~~ values, and ~~if~~ when a month ~~has~~ was missing more than 7 daily ~~missing~~ values, ~~it~~ that month was classified as a missing value (Sun et al., 2016; Li et al., 2015). ~~The~~ For the annual anomalies, ~~are the average of~~ the monthly anomalies were averaged for the entire year. The anomalies in the warm seasons ~~are~~ were the averages of the monthly anomalies from May to October, and the anomalies in the cold seasons ~~are~~ were the averages of the monthly anomalies from November to the next April.

带格式的: 字体: 倾斜

2.2 Methods

~~A linear regression model (see Eq. (1)) was used to calculate the trend of the climate variables and can be expressed as:~~

$$\cancel{y = a \cdot x + b \qquad (1)}$$

~~Where~~ where ~~*x* is time, *y* is the time series of the monthly anomalies of climate variables, and *a* and *b* are the trend and intercept, respectively, regressed using the least-squares method.~~

带格式的: 缩进: 首行缩进: 0 字符

As shown in Fig~~.~~ 1, the spatial distribution of the weather stations ~~over Mainland~~throughout China is extraordinarily asymmetric and the density of weather stations in ~~East~~ east China is far greater than that in ~~West~~ west China. We used the area-weight average method to reduce these biases when calculating the national mean. First, we divided the study region into 1° × 1° grids (see Fig~~.~~ S2) for a total ~~; there are~~ 953 grids covering China. Second, we assigned all selected stations to the grids~~; there are~~, and this resulted in 627 grids ~~with~~ containing stations, ~~accounting~~ which accounted for 65.79% of the total. Finally, the grid box value ~~is taken to be~~was the average of all ~~of the~~ stations ~~on~~ in the grid, and the national mean ~~is~~ was the area-weight average of all ~~of the~~ effective grids (Jones and Moberg, 2003).

The linear trends reported in this study were calculated ~~by~~via ~~a~~ linear regression based on the monthly anomalies of T, R_s, and P. Two national mean trends were calculated from the anomalies of the grids. In the first method (Method I), ~~the least square method.~~ ~~Based on the anomalies of grids, there are two common ways to calculate the national mean trends of the variables in China. The first method (Method I) calculates~~ the national mean monthly anomalies ~~by~~ were calculated us~~tak~~ing the area-weight of ~~every~~ each grid first, and then ~~calculates~~ the national mean trend based on the time series of the national average anomalies was calculated. ~~The~~ In the second method (Method II), ~~calculates~~ the trend at ~~every~~ each grid was calculated first, and then the national mean trend ~~over China is the area-weighted average value of the~~was calculated from the grid trends ~~on all of the grids~~.

In our study, we calculated the national mean trends of the temperatures using Method I and II because ~~both methods as~~ both methods ~~are widely~~ have been used in ~~the existing~~previous studies (Gettelman and Fu, 2008). ~~Same~~ The results for the two methods are ~~derived from those two methods if~~expected to be the same when the time series of all grids is ~~integral~~ integrated and ~~have no missing~~ data are not missing (Zhou et al., 2009); ~~.~~ ~~However~~however, when data are missing, small differences may occur (See Table 1). As shown in Table 1, the absolute value of the difference between Method I and Method II ranged from 0.011 to 0.033 °C 10yr^{-1}, which represented 3.4% to 14.3%

~~of the trends (using the results of Method I as the reference). For purposes of clarification, the trends derived from Method I are discussed in the main text, whereas the results from both methods are shown in Table 1.~~as noted, we selected 1,977 stations (see Fig. 1) that the valid data of observation records are longer than 30 years during the period 1960-2003, which is a reasonable compromise between the integrity of the observation records and the spatial coverage. The missing data in the time series for some grids results in a little difference between the results of these two methods. To avoid misunderstanding, the trends derived from Method I was discussed in the main text, but results from two methods were shown in Table 1.~~

[illegible] (Roy and Haigh, 2011) of the monthly anomalies using the following equation~~. This can be expressed as~~:

$$T = \quad S_{R_s} \cdot R_s + S_P \cdot P + c + \varepsilon \cancel{z = a \cdot x + b \cdot y + c + \varepsilon}$$

(~~2~~1)

where ~~z~~ T represents the monthly anomalies of $T_{s\text{-}max}$, $T_{s\text{-}min}$, $T_{a\text{-}max}$, and $T_{a\text{-}min}$; S_{Rs} and S_P are the sensitivities of the temperatures to R_s and P ~~***x*** and ***y*** are the monthly anomalies of the SSR and precipitation~~, respectively; ~~***a*** and ***b*** are the corresponding sensitivities of the temperatures to SSR and precipitation, respectively;~~ ***c*** is constant term; and ***ε*** indicates the residuals of the equation. The coefficients of determination (R^2) for the multilinear regression equation (Eq (1)) are shown in Fig S3, and they indicate the portion of the variance of T that could be attributed to that of R_s and P. High coefficients of determination were obtained, which showed that the linear regression performed well, particularly for South China and the North China Plain. To separate the contributions of R_s and P, we further calculated the partial correlation coefficients between R_s and T (or P and T), which are shown in Fig S4 and Fig S5.

To ~~adjust~~ determine the effect of R_s/P~~for the impact of SSR and precipitation~~ on the analyzed temperatures, we removed their effects from their original time series of $T_{s\text{-}max}$ and $T_{a\text{-}max}$ based on the multilinear relationship calculated in Eq (1). Then, we calculated the trends from both the original and adjusted time series. By comparing the derived trends of the original and adjusted time series, we quantitatively assessed the effect of R_s/P on $T_{s\text{-}max}$ and $T_{a\text{-}max}$, particularly for the spatiotemporal pattern of their trends.~~we took **x** as a time series of SSR and **y** as a time series of precipitation, while **a** and **b** are the sensitivities of the climate variables to changes in SSR and precipitation, respectively. The method of adjusting for the impact of SSR and precipitation is expressed as~~

$$\cancel{T_{adjusted} = T_{raw} - a \cdot x - b \cdot y \qquad (5)}$$

~~where $T_{adjusted}$ indicates the value of the climate variables after adjusting for the~~

~~impact of SSR and precipitation and T_{raw} is the value of the climate variables in the raw data.~~

3. Results

3.1. Trends of surface temperature and air temperature

3.1.1 T~~he t~~emporal patterns in ~~the variabilities of the~~ temperature variabilitys

~~Figs. 2 and Figs. 3 show t~~The long-term changes in $T_{s\text{-}max}$ and $T_{a\text{-}max}$ and ~~,~~ $T_{s\text{-}min}$ and $T_{a\text{-}min}$ from 1960 to 2003 are shown in Fig 2 and Fig 3, respectively. In addition to the annual variability (Fig~~s.~~ 2a and Fig~~s.~~ 3a), ~~we analyzed~~ the ~~variabilities of the~~ temperature variabilitys in both ~~the~~ warm seasons (May-October~~) (~~; Fig~~s.~~ 2b and Fig~~s.~~ 3b) and ~~the~~ cold seasons (November to the following April~~) (~~; Fig~~s.~~ 2c and Fig~~s.~~ 3c) were analyzed. In the annual records, all ~~of the~~ temperatures ~~showed~~ exhibited an obvious warming trend ~~over~~ throughout China (Fig~~s.~~ 2a and Fig~~s.~~ 3a).

As shown in Table 1, the national mean warming rate from 1960 to 2003 for $T_{s\text{-}max}$ was 0.227±0.091 °C 10yr^{-1} (95% confidence level) and ~~*the rate for*~~ $T_{a\text{-}max}$ was 0.167±0.068 °C 10yr^{-1} (95% confidence level)~~from 1960 to 2003~~. The warming rate of $T_{a\text{-}max}$ based on the 1,977 stations examined in ~~this paper~~the current study was ~~a little~~slightly higher than ~~both that of~~ the global average (0.141 °C 10yr^{-1}) from 1950 to 2004 (Vose et al., 2005) and ~~that~~ the rate obtained from ~~of~~ a previous analysis ~~of China~~

带格式的: 字体: 倾斜

带格式的: 字体: 倾斜

带格式的: 字体: 倾斜

带格式的: 字体: 倾斜

带格式的: 字体: 倾斜

带格式的: 字体: 倾斜

(0.127 °C 10yr^{-1}) of temperatures from 1955 to 2000 based on 305 stations in China (Liu et al., 2004). Additionally, the increases in

~~The seasonal contrasts of warming of T_{a-max} and T_{s-max} are important. T_{s-max} had an average rate of 0.172 °C 10yr^{-1} in the warm seasons and 0.354 °C 10yr^{-1} in the cold seasons. For T_{a-max}, it was 0.091 °C 10yr^{-1} and 0.294 °C 10yr^{-1} in the warm and cold seasons, respectively. The increases in~~ T_{s-max} and T_{a-max} in the cold seasons were much larger than those in the warm seasons, which is consistent with previous studies of China and other regions (Shen et al., 2014; Vose et al., 2005; Ren et al., 2005).

Similarly, the warming rates of T_{s-min} and T_{a-min} in the warm seasons were ~~clearly~~ also clearly lower than those in the cold seasons~~ too~~. As shown in Fig 3, T_{s-min} increased by 0.315±0.058 °C 10yr^{-1} (95% confidence level) and T_{a-min} increased by 0.356±0.0057 °C 10yr^{-1} (95% confidence level) (see Fig 3a) from 1960 to 2003.~~As shown in Figs. 3, T_{s-min} increased by 0.315 °C 10yr^{-1} and T_{a-min} increased by 0.356 °C 10yr^{-1} (see Figs. 3a) from 1960 to 2003.~~ The warming trend of T_{a-min} is generally consistent with earlier studies (Shen et al., 2014; Li et al., 2015; Liu et al., 2004); however, ~~it~~ these trends ~~is~~ are considerably larger than ~~that~~ the rates reported for the global average (0.204 °C 10yr^{-1}) (Vose et al., 2005). For the seasonal scales, the warming rate of T_{s-min}/T_{a-min} ~~increased at a rate of 0.221 °C 10yr^{-1} in the warm seasons~~

带格式的: 字体: 倾斜

带格式的: 字体: 倾斜

带格式的: 字体: 倾斜

带格式的: 字体: 倾斜

带格式的: 字体: 倾斜

带格式的: 字体: 倾斜

带格式的: 字体: 倾斜

带格式的: 字体: 倾斜

~~and 0.447 °C 10yr^{-1}~~ in the cold seasons ~~from~~ was almost double that of the warm seasons from 1960 to 2003 (see Table 1). ~~$T_{a\text{-}min}$ increased at rates of 0.245 °C 10yr^{-1} and 0.505 °C 10yr^{-1} in the warm and cold seasons, respectively.~~

~~On a national average scale, all temperatures increased from 1960 to 2003.~~ The warming rate of $T_{s\text{-}min}$ ($T_{a\text{-}min}$) was significantly faster than that of $T_{s\text{-}max}$ ($T_{a\text{-}max}$) and the warming rates of all temperatures in the cold seasons were ~~generally~~ substantially ~~higher~~ greater than those in the warm seasons~~. These basic characteristics of the temperature changes are consistent with previous studies on global or regional scales~~ (Li et al., 2015; Liu et al., 2004; Easterling et al., 1997)~~. (Hartmann et al., 2013)~~. Although previous studies have indicated that the microclimate (e.g. urban heat island) has a larger effect on minimum temperatures because of the lower and more stable boundary layer at night (Zhou and Ren, 2011; Christy et al., 2009), many investigators argue that variability in R_s is the primary reason for the daily contrast in warming rates (Sanchez-Lorenzo and Wild, 2012; Makowski et al., 2009). ~~(Liu et al., 2004; Karl et al., 1993)However, there remain slight differences between our results and previous studies with respect to the temperature warming rates, which might have several causes.~~

~~The number of stations used in our study is much greater in previous studies, which has led to better spatial coverage and a better representation of our analytical result. In~~

3.1.2. ~~The s~~Spatial patterns in ~~the variabilities for the~~ temperature variabilitys

As shown in Fig~~s.~~ 4, ~~demonstrates a~~ clear spatial heterogeneity was demonstrated in the warming rates for $T_{s\text{-}max}$ and $T_{a\text{-}max}$ ~~over~~ in China from 1960- to 2003. T~~$T_{s\text{-}max}$ and $T_{a\text{-}max}$ increased at high rate and t~~he trends of $T_{s\text{-}max}$ and $T_{a\text{-}max}$ were statistically ~~significant~~ higher ~~in~~ for the Tibet Plateau, and Northwest and Northeast China (see Fig~~s~~ S~~3~~6)~~. However, $T_{s\text{-}max}$ and $T_{a\text{-}max}$ had a relative lower warming rate in the~~ compared with the North China Plain and South China~~, –~~. ~~and $T_{s\text{-}max}$ even showed cooling~~ Cooling trends in $T_{s\text{-}max}$ even detected for the Sichuan ~~Plain~~Basin, the Yangtze River Delta, and the Pearl River Delta. Lower ~~warming~~ rates of warming of $T_{a\text{-}max}$ in South China and the North China Plain ~~had~~ have also been previously reported ~~in multiple previous studies~~ (Liu et al., 2004; Li et al., 2015).

~~For~~ The warming rates of $T_{s\text{-}max}$ and $T_{a\text{-}max}$~~, the warming rates of~~ in South China and the North China Plain in the warm seasons were considerably lower than those in the cold seasons, ~~resulting~~ which resulted in ~~a more obvious~~stronger spatial heterogeneity in the warm seasons (Fig~~s.~~ 4b and 4h). ~~However, the warming rates of both $T_{s\text{-}max}$ and $T_{a\text{-}max}$ in the Sichuan Basin and the Pearl River Delta were lower in the cold seasons than in the warm seasons. Despite of T~~the spatial and seasonal patterns of

带格式的: 字体: 倾斜
带格式的: 字体: 倾斜
带格式的: 字体: 倾斜
带格式的: 字体: 倾斜
带格式的: 字体: 倾斜
带格式的: 字体: 倾斜
带格式的: 字体: 倾斜
带格式的: 字体: 倾斜
带格式的: 字体: 倾斜, 下标
带格式的: 字体: 倾斜
带格式的: 字体: 倾斜
带格式的: 字体颜色: 文字 1

T_{a-max} were similar, although they were not as~~clearly~~ similar ~~to~~ as the ~~those~~ patterns of T_{s-max}. The spatial contrast in the trends between ~~*For T_{a-max}, both the seasonal asymmetry and the spatial heterogeneity of the warming trend were less than those of T_{s-max}.*~~

~~*For*~~ T_{s-min} and T_{a-min} was much less than that between T_{s-max} and T_{a-max}~~,~~, although a strong dependence on latitude was observed ~~the warming rates were highest in North China and generally decreased from north to south~~ (Fig~~s.~~ 4d and 4j). ~~The average warming rates of T_{s-min} and T_{a-min} in the cold seasons (Figs. 4f and 4l) were faster than those in the warm seasons (Figs. 4e and 4k). This variation of warming rate with latitudes have~~This dependence has been successfully ~~been~~ attributed to amplified dynamics ~~amplification~~ (Wallace et al., 2012; Ding et al., 2014). ~~In this study, we focus on the spatial heterogeneity of the warming rates at similar latitudes and diurnal contrast of the warming rates.~~

~~By contrasting the annual variation and spatial pattern of trends, we found that~~The correlation between T_s and T_a was highly ~~had an extremely~~ significant. ~~correlation with each other.~~ Based on the time series of the national mean yearly anomalies (see Fig~~s.~~ 2 and Fig~~s.~~ 3), the correlation coefficient~~s~~ between T_{s-max} and T_{a-max} ~~were~~ was 0.877 ~~,~~ ~~0.799, and 0.921 on the annual, warm, and cold seasonal scales, respectively. The~~

带格式的: 字体: 倾斜, 字体颜色: 文字 1
带格式的: 字体颜色: 文字 1
带格式的: 字体颜色: 文字 1
带格式的: 字体: 倾斜, 字体颜色: 文字 1
带格式的: 字体颜色: 文字 1
带格式的: 字体: 倾斜
带格式的: 字体: 倾斜
带格式的: 字体: 倾斜
带格式的: 字体: 倾斜
带格式的: 字体: 倾斜
带格式的: 字体: 倾斜

~~correlations~~ and between $T_{s\text{-}min}$ and $T_{a\text{-}min}$ ~~were~~ was 0.976 ~~, 0.969, and 0.977~~ on the annual~~, warm, and cold seasonal~~ scale ~~s, respectively. In the spatial pattern of the trends~~ In the spatial pattern of the trends (Fig~~s.~~ 4), the correlation coefficient~~s~~ between $T_{s\text{-}max}$ and $T_{a\text{-}max}$ ~~were~~ was 0.488 and ~~, 0.465, and 0.522 on the annual, warm, and cold seasonal scales, respectively. Those~~ between $T_{s\text{-}min}$ and $T_{a\text{-}min}$ ~~were~~ was 0.638 ~~, 0.670, and 0.594~~ on the annual~~, warm, and cold seasonal~~ scale~~s, respectively~~. All of these correlations between T_s and T_a were significant at the 95% significance level, which indicated a close relation between T_s and T_a for both interannual fluctuations and secular trends.

~~In summary, T_s had a significant correlation with Ta both in annual variation (Figs. 2 and Figs. 3) and in long-term trends (Figs. 4), indicating that T_s observational records are reliable for climate change research. However, t~~The correlation between $T_{s\text{-}min}$ and $T_{a\text{-}min}$ was significantly higher than that between $T_{s\text{-}max}$ and $T_{a\text{-}max}$. $T_{s\text{-}min}$ is closely related to the land~~-~~–atmosphere longwave wave radiation balance ~~during the nighttime~~at night, which is closely ~~related~~ associated ~~to~~ with the atmospheric greenhouse effect (Dai et al., 1999). During the day~~time~~, T_s is directly determined by the land surface energy balance, i.e., the incoming energy (including ~~SSR~~R_s) and atmospheric longwave radiation (Wang and Dickinson, 2013a), and it is ~~partitions~~ partitioned into latent and sensible heat fluxes (Zhou and Wang, 2016). ~~Despite~~ Although ~~*its*~~ T_a is ~~dependence~~ dependent on the land-atmosphere

带格式的: 字体: 倾斜
带格式的: 字体: 倾斜
带格式的: 字体: 倾斜
带格式的: 字体: 倾斜
带格式的: 字体: 倾斜
带格式的: 字体: 倾斜
带格式的: 字体: 倾斜
带格式的: 字体: 倾斜
带格式的: 字体: 倾斜
带格式的: 字体: 倾斜
带格式的: 下标
带格式的: 字体: 倾斜
带格式的: 字体: 倾斜, 下标

sensible heat flux, it ~~T_a~~ is also ~~impacted~~ affected by local and/or large-scale circulation. ~~So~~Thus, the changes ~~of~~ in the land surface energy balance caused by ~~SSR~~R_s and ~~*precipitation*~~ P have different levels of effect on T_s and T_a during the day, which most likely ~~causes~~ caused ~~a~~ the lower correlation between $T_{s\text{-}max}$ and $T_{a\text{-}max}$ than that between $T_{s\text{-}min}$ and $T_{a\text{-}min}$.

3.2. ~~The impact of~~Effect of ~~*surface solar radiation*~~R_s and ~~*precipitation*~~ P on temperatures

3.2.1 Effect of R_s~~Impact of surface solar radiation~~

~~-~~As shown in Fig~~s.~~ S4, ~~shows that SSR~~R_s ~~had~~ is closely ~~an important relationship~~linked with $T_{s\text{-}max}$ and $T_{a\text{-}max}$ but not with $T_{s\text{-}min}$ and $T_{a\text{-}min}$, and the correlation ~~and $T_{a\text{-}min}$~~between $T_{s\text{-}max}$~~.~~ and R_s was higher than that between $T_{a\text{-}max}$ and R_s~~The national mean of the partial correlation coefficients between SSR and $T_{s\text{-}max}$ is 0.552 and 98.9% of the stations are statistically significant at the 1% level. Meanwhile, the national mean of the partial correlation coefficients between SSR and $T_{a\text{-}max}$ is 0.441, and 95.4% of the stations are statistically significant at the 1% level. This relationship is stronger in South China and on the North China Plain, i.e., it reaches 0.810 for $T_{s\text{-}max}$ and 0.765 for $T_{a\text{-}max}$.~~

带格式的: 字体: 倾斜
带格式的: 下标
带格式的: 字体: 倾斜
带格式的: 字体: 倾斜
带格式的: 字体: 倾斜
带格式的: 字体: 倾斜
带格式的: 字体: 倾斜
带格式的: 字体: 倾斜
带格式的: 字体: 倾斜
带格式的: 字体: 倾斜
带格式的: 字体: 倾斜, 下标
带格式的: 字体: 倾斜
带格式的: 字体: 小四, 加粗
带格式的: 下标
带格式的: 字体: 倾斜
带格式的: 字体: 倾斜
带格式的: 字体: 倾斜
带格式的: 字体: 倾斜

[illegible] warm seasons ~~is~~ was higher than that in the cold seasons, and this correlation was stronger in South China and the North China Plain.~~the national mean partial correlation coefficients for the warm and cold seasons are 0.579 and 0.498 for $T_{s\text{-}max}$ and 0.544 and 0.386 for $T_{a\text{-}max}$, respectively, consisting with the seasonal cycle of SSR intensity over China.~~

~~Spatially, overall, the partial correlation coefficients between $T_{s\text{-}max}$ and $T_{a\text{-}max}$ and SSR are higher in South China than in North China (see Figs. 5a–5c and 5g–5i). South of 35° N, the national mean of the partial correlation coefficients between $T_{s\text{-}max}$ ($T_{a\text{-}max}$) and SSR is 0.654 (0.552), whereas that between $T_{s\text{-}max}$ ($T_{a\text{-}max}$) and SSR is just 0.417 (Shen et al., 2014) north of 35° N. During daytime, T_s and T_a is largely determined by how much energy is used to evapotranspiration.~~ S~~In s~~outh China has high~~where~~ soil moisture~~ is high,~~; therefore, the relationship between the energy used for evapotranspiration and ~~is near linearly related to SSR~~R_s is approximately linear (Wang and Dickinson, 2013b; Zhou et al., 2007). However, northwest China presents dry soil over most of the year; thus the energy used for evapotranspiration is more dependent on ~~*precipitation in the northwest China where the soil is dry during most time of a year*~~*P*. As a result, the energy available for heating the surface and air temperatures is not as~~so~~ closely correlated with ~~*SSR*~~R_s. Therefore, the correlation coefficients between

带格式的: 下标

带格式的: 字体: 倾斜

带格式的: 字体: 倾斜

带格式的: 下标

[illegible]

To quantify the ~~impact~~ effect of ~~SSR~~R_s on temperature, the sensitivity of the studied temperatures to changes in ~~SSR~~R_s ~~has been~~was calculated (Eq. (~~2~~1)). As shown in ~~Figs. 6~~Fig S7 shows, T_{s-max} was the most sensitive to ~~SSR~~R_s, followed by T_{a-max}, and the~~ir~~ national means ~~were~~ for T_{s-max} was 0.092±0.018 °C (W m^{-2})$^{-1}$ (95% confidence level) and T_{a-max} was 0.035±0.010 °C (W m^{-2})$^{-1}$ (95% confidence level)~~, respectively~~. T_{s-min} and T_{a-min} were ~~insignificantly~~ not sensitive to ~~SSR~~R_s because these temperatures are primarily affected by ~~they primarily depend on~~ atmospheric longwave radiation ~~during the nighttime~~night.

Based on the above analysis, we calculated the ~~impact~~ effect of changes in ~~SSR~~R_s on the studied temperature~~s (see the Method Section)~~. From 1960 to ~~–~~2003, the calculations of the monthly anomalies at 1,977 stations indicated that the national mean rate of decreas~~ing ratee~~e of ~~SSR~~R_s was −1.502±0.42 W m^{-2} 10yr^{-1} (95% confidence level), ~~as calculated from monthly anomalies at 1,977 stations,~~ and the trend was significant in most regions ~~over~~ of China (see ~~Figs. S4~~Fig S8). Our ~~results~~ rate of decrease was ~~are~~ considerably less than the global average ~~dimming~~ diminishing rate (form approximately −2.3 ~~–~~to −5.1 W m^{-2} 10yr^{-1}) between the 1960s and the 1990s (Gilgen et al., 1998; Liepert, 2002; Stanhill and Cohen, 2001; Ohmura, 2006) and the

带格式的: 下标
带格式的: 下标
带格式的: 字体: 倾斜
带格式的: 下标
带格式的: 字体: 倾斜
带格式的: 字体: 倾斜
带格式的: 字体: 倾斜, 下标
带格式的: 字体: 倾斜
带格式的: 字体: 倾斜
带格式的: 下标
带格式的: 下标
带格式的: 下标

national mean dimming rate across China (from approximately −2.9 to~~∼~~ −5.2 W m^{-2} 10yr^{-1}) between the 1960s and the 2000s based on radiation station observations (Che et al., 2005; Liang and Xia, 2005; Shi et al., 2008; Wang et al., 2015a).

As noted in the data section, the sensitivity drift~~ing~~ and replacement of ~~the~~ instruments used for the ~~SSR~~R_s observations ~~results~~ resulted in a significant homogenization ~~in~~ of the station~~s~~ observation records (Wang, 2014; Wang et al., 2015a), which ~~causes~~ introduced considerable ~~a great~~ uncertainty ~~in~~ to the trend ~~–~~estimations. Tang et al. (2011) used quality-controlled observational data from 72 stations and two radiation models based on 479 stations to determine ~~both~~ that the ~~dimming~~ rate in~~over~~ China ~~is~~ decreased from approximately −2.1 ~~∼~~to −2.3 W m^{-2} 10yr^{-1} during 1961-2000, and ~~that the~~they also showed that ~~SSR~~R_s values ~~has~~ have remained ~~been~~ essentially unchanged since 2000.~~;~~ ~~this~~ These findings ~~is~~ are generally consistent with our results.

~~Due to~~Because of the decreasing trend in ~~SSR~~R_s, the national mean warming trends of $T_{s\text{-}max}$ and $T_{a\text{-}max}$ decreased by 0.139 °C 10yr^{-1} and 0.053 °C 10yr^{-1}, respectively~~, in the national mean~~. Spatially, the decreasing rate of ~~SSR~~R_s in South China and the North China Plain was significantly higher than that in other regions, ~~especially~~ particularly in the warm seasons (~~Figs. 7~~Fig 5b). Therefore, the cooling effect of decreasing ~~SSR~~R_s on $T_{s\text{-}max}$ and $T_{a\text{-}max}$ was more significant in South China and the

带格式的: 下标
带格式的: 下标
带格式的: 下标
带格式的: 字体: 倾斜
带格式的: 字体: 倾斜
带格式的: 下标
带格式的: 下标
带格式的: 字体: 倾斜
带格式的: 字体: 倾斜

China North Plain, and it resulted~~ing~~ in significantly lower warming rates of $T_{s\text{-}max}$ and $T_{a\text{-}max}$ in those regions ~~there~~ than in the other regions (see Figs. 4). The spatial consistency between the decreasing ~~SSR~~R_s trend and the ~~warming~~ slowdown of $T_{s\text{-}max}$ ~~(~~/$T_{a\text{-}max}$~~)~~ ~~implies~~ warming implied that variations in ~~SSR~~R_s ~~is~~ were the primary reason for the spatial heterogeneity of the warming rate in $T_{s\text{-}max}$ ~~(~~/$T_{a\text{-}max}$~~)~~.

3.2.2 Effect of *P* ~~Impact of Precipitation~~

As shown in Fig S5,~~Figs. 8a~~ a ~~shows that there is a~~ significant negative correlation was detected between $T_{s\text{-}max}$ and ~~*precipitation*~~*P*, and~~;~~ the ~~national~~ correlation was more significant in the warm seasons than in the cold seasons. *P*~~mean of the partial correlation coefficients is −0.323, and 99.3% of the stations are statistically significant at the 1% level. Seasonally, the correlation is stronger in the warm seasons (regional mean: −0.405) than in the cold seasons (regional mean: −0.276). In warm seasons, the correlation in North China (regional mean: −0.459) is clearly stronger than in South China (regional mean: −0.365). In cold seasons, the correlation is highest on the Southwestern Yunnan-Guizhou Plateau and in most regions of North China (regional mean: −0.305) (Figs. 8b and 8c), whereas it was~~ is ~~relatively weak in Southeastern China, the Tibet Plateau, Dzungaria, the Tarim Basin, and some regions of Northeastern China (regional mean: −0.117). The correlations between T~~$_{a\text{-}max}$ ~~and precipitation had~~

带格式的: 字体: 倾斜
带格式的: 字体: 倾斜
带格式的: 下标
带格式的: 字体: 倾斜
带格式的: 字体: 倾斜
带格式的: 下标
带格式的: 字体: 倾斜
带格式的: 字体: 倾斜
带格式的: 字体: 倾斜
带格式的: 字体: 倾斜
带格式的: 字体: 倾斜

have ~~similar spatial and seasonal patterns (Figs. 8g–8i) too, and 35.4% of the stations had a correlation between $T_{a\text{-}max}$ and the precipitation that was~~are ~~statistically significant at the 1% level; these were~~ are ~~primarily concentrated in arid and semiarid regions of China (regional mean: −0.167) (Figs. 8e–8f and 8j–8l).~~

~~Precipitation~~ ~~has a~~ negatively ~~relationship~~ correlated with temperature because ~~*precipitation*~~ *P* ~~can~~ reduces temperatures by increasing the surface evaporative cooling (Dai et al., 1997; Wang et al., 2006). ~~The impact of precipitation on temperature was~~ is ~~higher in the warm seasons over China, which is consistent with seasonal changes in the correlation between $T_{s\text{-}max}$ and $T_{a\text{-}max}$ and precipitation (see Figs. 8b–8c and 8h–8i).~~T

~~T~~he national mean sensitivities of $T_{s\text{-}max}$ and $T_{a\text{-}max}$ to ~~*precipitation*~~ *P* were −0.321±0.098 °C 10 mm^{-1} and −0.064±0.054 °C 10 mm^{-1} (95% confidence level), respectively. As shown in ~~Figs. 9~~Fig S9, ~~there were apparent~~ seasonal and spatial changes in the sensitivity of $T_{s\text{-}max}$ and $T_{a\text{-}max}$ to ~~*precipitation*~~ *P* were apparent (~~Figs. 9~~Fig S9a–~~9~~c and Fig S9~~9~~g–~~9~~i). ~~In warm seasons, these sensitivities were highest in the Tibet Plateau, the Loess Plateau, the Inter Mongolia Plateau, Dzungaria, and the Tarim Basin (Figs. 9b and 9h). In cold seasons, the distribution of regions with high sensitivity extended to all of North China and Southwest China (Figs. 9c and 9i). Overall, t~~The sensitivities of $T_{s\text{-}max}$ ~~(~~/$T_{a\text{-}max}$~~)~~ were significantly higher in arid regions (dry seasons)

带格式的: 字体: 倾斜

带格式的: 字体: 倾斜

带格式的: 字体: 倾斜

带格式的: 字体: 倾斜

带格式的: 字体: 倾斜

带格式的: 字体: 倾斜

带格式的: 字体: 倾斜

带格式的: 字体: 倾斜

带格式的: 字体: 倾斜

than ~~in~~ humid~~ity~~ regions (rainy seasons) (Wang and Dickinson, 2013b). ~~In contrast~~As expected, T_{s-min} and T_{a-min} were both less sensitive to variations in the ~~*precipitation*~~*P*.

~~As Figs. 10 shows, during 1960-2003, t~~The trend in ~~*the precipitation*~~*P* from 1960 to 2003 over the 1,977 stations ~~had~~ showed obvious spatial heterogeneities. ~~China's precipitation during this period showed a~~A slight increasing trend in *P* was observed in China during this period at ~~with an increasing~~ rate of 0.112±0.718 mm 10yr^{-1} (95% confidence level). An increasing ~~*Precipitation*~~ *P* trend was observed in ~~Northwestern~~ northwestern China and ~~Southeastern~~ southeastern China ~~experienced an increasing trend~~, whereas a decreasing trend was observed in the ~~precipitation in the~~ North China Plain, the Sichuan Basin, and parts of ~~Northeastern~~ northeastern China ~~experienced a decreasing trend~~. However, the ~~*trend of precipitation*~~*P* trends ~~was~~ were not ~~in~~significant in most regions (see ~~Figs. S4~~Fig S8). Variations in ~~*precipitation*~~ *P*~~had~~ significantly differed by season~~al differences~~ (see ~~Figs. 10~~Fig 6b and Fig 6~~10~~c). The seasonal and spatial ~~characteristics~~ variations in~~of~~ ~~*these precipitation variations*~~*P* are consistent with those ~~identified in~~of previous studies (Zhai et al., 2005; Wang et al., 2015b).

~~Therefore, f~~For T_{a-max} and T_{s-max}, ~~the reduction in precipitation aggravated~~ the warming trend in the North China Plain, the Sichuan Basin, and parts of ~~Northeastern~~ northeastern China was aggravated by the reduction in *P*, whereas the warming trend

带格式的: 字体: 倾斜
带格式的: 字体: 倾斜
带格式的: 字体: 倾斜
带格式的: 字体: 倾斜
带格式的: 字体: 倾斜
带格式的: 字体: 倾斜
带格式的: 字体: 倾斜
带格式的: 字体: 倾斜
带格式的: 字体: 倾斜
带格式的: 字体: 倾斜

~~increase~~ in ~~precipitation primarily slowed the warming trend in N~~northwestern China and ~~on~~ in the Mongolian Plateau were slowed by increases in *P* (~~Figs. 10~~Fig 6d). ~~On~~ For the national average, the ~~impact~~ effect of increasing ~~*precipitation*~~ *P* resulted in decreases in the warming trends of T_{s-max} and T_{a-max} ~~being decreased~~ by −0.007 °C 10yr^{-1} and −0.002 °C 10yr^{-1}, respectively. However, ~~compared to SSR,~~ the ~~impact~~ effect of ~~*precipitation*~~ *P* on T_{s-max} was ~~smaller by~~ approximately an order of magnitude less than that of R_s. ~~For T_{s-min} and T_{a-min}, the impact of changes in precipitation was insignificant.~~

3.3. Trends of surface and air temperature after adjusting for the effect of ~~SSR~~R_s and ~~*precipitation*~~*P*

Based on the above analysis of the ~~impact~~ effect of ~~SSR~~R_s and ~~*precipitation*~~ *P* on temperatures, we found that ~~the~~ variations ~~of~~ in ~~SSR~~R_s and ~~*precipitation*~~ *P* had little effect on T_{s-min} and T_{a-min}. However, R_s and *P* had important effect on the trends of T_{s-max} and T_{a-max} (see Fig S3), particularly in central and South China, where *T* was more closely related to R_s (see Fig S4). ~~Therefore~~Therefore, ~~we~~ only the effects of R_s and *P* on T_{s-max} and T_{a-max} were analyzed~~analyzed their impact on T_{s-max} and T_{a-max}~~. After adjusting for the ~~impact~~ effect of ~~SSR~~Rs and ~~*precipitation*~~ *P* (~~Figs. 11~~Fig 7), the warming rates of T_{s-max} and T_{a-max} increased by 0.146 °C 10yr^{-1} (64.3%) and 0.055 °C

10yr^{-1} (33.0%), respectively.

~~After adjusting~~Additionally, the increasing amplitude of warming rates in the warm seasons was significantly higher than that in the cold seasons, which resulted in ~~the~~ a seasonal contrast in warming rates, with ~~of~~ $T_{s\text{-}max}$ and $T_{a\text{-}max}$ decreasing~~ed~~ by 45.0% and 17.2% respectively (see Table 1). ~~The national mean warming rate of $T_{s\text{-}max}$ increased by 0.178 °C 10yr^{-1} (103.1%) in the warm seasons and 0.086 °C 10yr^{-1} (27.2%) in the cold seasons. For $T_{a\text{-}max}$, the warming rate increased by 0.069 °C 10yr^{-1} (76.4%) in the warm seasons and 0.034 °C 10yr^{-1} (11.7%) in the cold seasons.~~

~~After adjusting for the impact of SSR and *precipitation*, the difference in warming rates between $T_{a\text{-}max}$ and $T_{a\text{-}min}$ changed from 0.190 to 0.134 °C 10yr^{-1}, a decrease of 29.1%, and the difference between $T_{s\text{-}max}$ and $T_{s\text{-}min}$ changed from 0.088 to 0.058 °C 10yr^{-1}, a decrease of 33.0%.~~

More importantly, after adjusting for the ~~impact~~ effect of ~~SSR~~R_s and ~~*precipitation*~~*P*, the spatial coherence of the warming rates of $T_{s\text{-}max}$ and $T_{a\text{-}max}$ in South China and the North China Plain clearly improved (~~Figs. 12~~Fig 8). The regional differences ~~between~~ among the North China Plain, South China, and other regions in China ~~shrank~~ significantly ~~due to~~decreased because of the increase in ~~the~~ warming rates in South China and the North China Plain. ~~In addition~~Additionally, the warming trends

带格式的: 字体: 倾斜

带格式的: 字体: 倾斜

带格式的: 字体: 倾斜

带格式的: 下标

带格式的: 字体: 倾斜

带格式的: 字体: 倾斜

带格式的: 字体: 倾斜

of T_{s-max} and T_{a-max} became more statistically significant in the North China Plain and South China (see ~~Figs. S5~~10).

To ~~further prove this~~clearly illustrate these changes, we selected two regions in China for further investigation: R1 primarily ~~includes~~ included the North China Plain and R2 primarily ~~includes~~ included the Loess Plateau ~~, as shown in~~(see ~~Figs. 13~~Fig 9a). Although t~~T~~hese regions share the same latitudes, ~~. However,~~ the trend for ~~SSR~~R_s were ~~showed~~ substantially different (see Fig 9b). ~~contrasting trends in the two regions (see Figs. 13b).~~

After adjusting for the ~~impacts~~ effect of ~~SSR~~R_s and ~~*precipitation*~~*P*, the annual trends ~~of~~ for T_{s-max} and T_{a-max} in R1 increased by 0.304 and 0.118 °C 10yr^{-1}, respectively, whereas ~~while~~ those in R2 ~~just~~ increased by only 0.025 and 0.016 °C 10yr^{-1}, respectively. Therefore, following the adjustment, ~~The~~ the differences in the warming rates of T_{s-max} and T_{a-max} between R1 and R2 ~~reduced~~ were significantly reduced ~~after adjusting~~ (see ~~Figs. 13~~Fig 9d).

~~Meanwhile~~Following the adjustment ~~,~~ in R1, the seasonal and diurnal differences in the warming rates of T_{s-max} and T_{a-max} ~~decreased~~ significantly decreased. ~~After adjusting, in R1, t~~The differences in warming rates between the warm seasons and cold seasons decreased by 68.7% for T_{s-max} and ~~decreased~~ by 50.8% for T_{a-max} after the

带格式的: 下标

带格式的: 下标

带格式的: 字体: 倾斜

带格式的: 字体: 倾斜

带格式的: 字体: 倾斜

带格式的: 字体: 倾斜

带格式的: 字体: 倾斜

带格式的: 字体: 倾斜

带格式的: 字体: 倾斜

带格式的: 字体: 倾斜

带格式的: 字体: 倾斜

adjustment. Additionally, t~~T~~he differences in the warming rates between $T_{s\text{-}max}$ and $T_{s\text{-}min}$ decreased by 93.4% and ~~that~~ between $T_{a\text{-}max}$ and $T_{a\text{-}min}$ decreased by 59.6% in R1. In R2, the adjustment did not significantly change the seasonal and diurnal differences in temperatures. ~~The seasonal and diurnal difference of temperatures in R2 had no significant changes after adjusting.~~ ~~All in all~~Overall, the trends ~~of~~ for R1 and R2 became more consistent ~~with each other~~ after adjusting ~~the~~ for difference in ~~SSR~~ R_s and ~~*precipitation*~~ P ~~between them~~ (see ~~Figs. 13~~Fig 9d).

4. Conclusions and Discussion

~~In China, despite the~~Although a general warming trends has been observed throughout China, ~~over the entire country,~~ the regional warming trends showed significant spatial and temporal heterogeneity. In this ~~paper~~study, we analyzed the spatial and temporal patterns of T_s and T_a from 1960 to 2003 and further analyzed and quantified the ~~impact~~ effects of ~~SSR~~ R_s and ~~*precipitation*~~ P on these temperatures. The ~~main~~ primary results of the study are as follows.

The national mean warming rates from 1960 to 2003 of $T_{s\text{-}max}$, $T_{s\text{-}min}$, $T_{a\text{-}max}$, and $T_{a\text{-}min}$ were 0.227±0.091, 0.315±0.058 ~~°C 10yr^{-1}~~, 0.167±0.068 ~~°C 10yr^{-1}~~, and 0.356±0.057 °C 10yr^{-1}, respectively~~,~~. ~~from 1960 to 2003.~~ The~~he warming rates of $T_{s\text{-}min}$ and $T_{a\text{-}min}$ were significantly greater than those of $T_{s\text{-}max}$ and $T_{a\text{-}max}$ (see Figs. 2 and Figs. 3).~~ ~~Warming~~ warming rates of $T_{s\text{-}max}$ and $T_{a\text{-}max}$ in South China and ~~on~~ the North

带格式的: 字体: 倾斜
带格式的: 字体: 倾斜
带格式的: 字体: 倾斜
带格式的: 字体: 倾斜
带格式的: 下标
带格式的: 字体: 倾斜
带格式的: 下标
带格式的: 字体: 倾斜
带格式的: 字体: 倾斜
带格式的: 字体: 倾斜
带格式的: 字体: 倾斜
带格式的: 字体: 倾斜
带格式的: 字体: 倾斜

China Plain were significantly lower than those in the other regions ~~(see Figs. 4).~~, and ~~The~~ the spatial heterogeneity in the warm seasons was greater than that in the cold seasons.

During the study period, the ~~SSR~~R_s value decreased by −1.502±0.042 W m^{-2} 10yr^{-1} (95% confidence level)~~in China~~, ~~with~~ and higher ~~dimming~~ diminishing rates were observed in South China and the North China Plain. Using a partial regression analysis, we found that ~~SSR~~R_s was the primary cause of the spatial patterns in the warming rates of $T_{s\text{-}max}$ and $T_{a\text{-}max}$.

After adjusting for the effect of R_s and P, the warming rates of $T_{s\text{-}max}$ and $T_{a\text{-}max}$ in South China and the North China Plain significantly increased and the regional differences in warming rates in China clearly decreased (see Fig 8). After the adjustments, the warming rates of $T_{s\text{-}max}$ and $T_{a\text{-}max}$ in the North China Plain increased by 0.304 and 0.118 °C 10yr^{-1}, respectively, whereas those on Loess Plateau increased only by 0.025 and 0.016 °C 10yr^{-1}, respectively. Therefore, the differences in warming rates of $T_{s\text{-}max}$ and $T_{a\text{-}max}$ between the North China Plain and the Loess Plateau were almost eliminated (see Fig 9d).

After adjusting for the effect of R_s and P, the warming trend of $T_{s\text{-}max}$ increased by 0.146 °C 10yr^{-1} and that of $T_{a\text{-}max}$ increased by 0.055 °C 10yr^{-1}. In addition, the trends of $T_{s\text{-}max}$ and $T_{a\text{-}max}$ became 0.373±0.068 and 0.222±0.062 °C 10yr^{-1} respectively.

带格式的: 下标

带格式的: 下标

带格式的: 字体: 倾斜

带格式的: 字体: 倾斜

Reduction in R_s resulted in decreases in the warming rates of T_{s-max} and T_{a-max} by 0.139 °C 10yr^{-1} and 0.053 °C 10yr^{-1}, respectively, which accounted for 95.0% and 95.8% of the total effect of R_s and P, respectively. For the seasonal contrast, the warming rates of T_{s-max} and T_{a-max} decreased by 45.0% and 17.2%, respectively. For the daily contrast, the warming rates of T_s and T_a decreased by 33.0% and 29.1%, respectively.~~After adjusting for the impact of SSR and precipitation, the warming trend of T_{s-max} increased by 0.146 °C 10yr^{-1} and that of T_{a-max} increased by 0.055 °C 10yr^{-1}. After adjustments, the trends of T_{s-max}, T_{s-min}, T_{a-max}, and T_{a-min} became 0.373 °C 10yr^{-1}, 0.315 °C 10yr^{-1}, 0.222 °C 10yr^{-1}, and 0.356 °C 10yr^{-1}. The reduction of SSR resulted in the warming rates of T_{s-max} and T_{a-max} decreasing by 0.139 °C 10yr^{-1} and 0.053 °C 10yr^{-1}, accounting for 95.0% and 95.8%, respectively, of the total impact of SSR and precipitation.~~

In addition to ~~SSR~~R_s and ~~*precipitation*~~P, temperatures~~'~~ warming rates may be affected by many other factors, such as land cover and land use changes~~,~~; ~~that~~ however those factors have not been discussed in this study ~~due to~~because of lack of data~~, i.e., land cover and land use~~ (Liu et al., 2005; Zhang et al., 2016). After adjusting for the ~~impact~~ effect of changes in ~~SSR~~R_s and ~~*precipitation*~~ P changes, the spatial differences in the warming trends clearly decreased; however, ~~some~~ certain regional differences remained. The warming rate of T_{s-max} in the Sichuan Basin remained significantly lower than that in other regions after adjusting for these ~~impacts~~effects. ~~In~~

带格式的: 下标

带格式的: 字体: 倾斜

带格式的: 下标

带格式的: 字体: 倾斜

带格式的: 字体: 倾斜

~~addition~~Additionally, the differences ~~north-south difference~~ in the warming rates of T_{s-min} and T_{a-min} between the northern and southern areas were not ~~cannot be~~ explained by the ~~impacts~~ effects of ~~SSR~~R_s and ~~*precipitation*~~P; ~~.~~ ~~Further~~ further study is ~~needed~~required.

Acknowledgements ~~This study was funded by t~~The National Natural Science Foundation of China (41525018 and 91337111) and the National Basic Research Program of China funded this study. The ~~latest day and night precipitation datasets, collected at approximately 2,100 meteorological stations in China from 1979 to 2014,~~land surface temperatures and sunshine duration datasets that include data from approximately 2,400 meteorological stations in China from 1960 to 2003, are obtained from the China Meteorological Administration (CMA, http://data.cma.gov.cn/data).

带格式的: 字体: 倾斜

带格式的: 字体: 倾斜

带格式的: 下标

带格式的: 字体: 倾斜

References

Ait-Mesbah, S., Dufresne, J. L., Cheruy, F., and Hourdin, F.: The role of thermal inertia in the representation of mean and diurnal range of surface temperature in semiarid and arid regions, Geophys Res Lett, 42, 7572-7580, 10.1002/2015gl065553, 2015.

Bounoua, L., Collatz, G. J., Sellers, P. J., Randall, D. A., Dazlich, D. A., Los, S. O., Berry, J. A., Fung, I., Tucker, C. J., Field, C. B., and Jensen, T. G.: Interactions between vegetation and climate: Radiative and physiological effects of doubled atmospheric CO2, J Climate, 12, 309-324, 10.1175/1520-0442(1999)012<0309:ibvacr>2.0.co;2, 1999.

Boyles, R. P., and Raman, S.: Analysis of climate trends in North Carolina (1949-1998), Environ Int, 29, 263-275, 10.1016/s0160-4120(02)00185-x, 2003.

Campbell, G. G., and VonderHaar, T. H.: Comparison of surface temperature minimum and maximum and satellite measured cloudiness and radiation budget, J Geophys Res-Atmos, 102, 16639-16645, 10.1029/96jd02718, 1997.

Cao, L., Zhu, Y., Tang, G., Yuan, F., and Yan, Z.: Climatic warming in China according to a homogenized data set from 2419 stations, Int J Climatol, 36, 4384-4392, 10.1002/joc.4639, 2016.

Che, H. Z., Shi, G. Y., Zhang, X. Y., Arimoto, R., Zhao, J. Q., Xu, L., Wang, B., and Chen, Z. H.: Analysis of 40 years of solar radiation data from China, 1961-2000, Geophys Res Lett, 32, 10.1029/2004gl022322, 2005.

Chen, H. S., Ma, H. D., Li, X., and Sun, S. L.: Solar influences on spatial patterns of Eurasian winter temperature and atmospheric general circulation anomalies, J Geophys Res-Atmos, 120, 8642-8657, 10.1002/2015jd023415, 2015.

Cheng, Z., Wang, S., Fu, X., Watson, J. G., Jiang, J., Fu, Q., Chen, C., Xu, B., Yu, J., Chow, J. C., and Hao, J.: Impact of biomass burning on haze pollution in the Yangtze River delta, China: a case study in summer 2011, Atmos. Chem. Phys., 14, 4573-4585, 10.5194/acp-14-4573-2014, 2014.

Christy, J. R., Norris, W. B., and McNider, R. T.: Surface Temperature Variations in East Africa and Possible Causes, J Climate, 22, 3342-3356, 10.1175/2008jcli2726.1, 2009.

带格式的: 缩进: 左侧: 0 厘米, 悬挂缩进: 2 字符, 首行缩进: -2 字符

Dai, A., DelGenio, A. D., and Fung, I. Y.: Clouds, precipitation and temperature range, Nature, 386, 665-666, 10.1038/386665b0, 1997.

Dai, A., Trenberth, K. E., and Karl, T. R.: Effects of clouds, soil moisture, precipitation, and water vapor on diurnal temperature range, J Climate, 12, 2451-2473, 10.1175/1520-0442(1999)012<2451:eocsmp>2.0.co;2, 1999.

Ding, Q., Wallace, J. M., Battisti, D. S., Steig, E. J., Gallant, A. J. E., Kim, H.-J., and Geng, L.: Tropical forcing of the recent rapid Arctic warming in northeastern Canada and Greenland, Nature, 509, 209-+, 10.1038/nature13260, 2014.

Duan, A., and Xiao, Z.: Does the climate warming hiatus exist over the Tibetan Plateau?, Sci. Rep, 5, 10.1038/srep13711, 2015.

Easterling, D. R., Horton, B., Jones, P. D., Peterson, T. C., Karl, T. R., Parker, D. E., Salinger, M. J., Razuvayev, V., Plummer, N., Jamason, P., and Folland, C. K.: Maximum and minimum temperature trends for the globe, Science, 277, 364-367, 10.1126/science.277.5324.364, 1997.

Falge, E., Reth, S., Bruggemann, N., Butterbach-Bahl, K., Goldberg, V., Oltchev, A., Schaaf, S., Spindler, G., Stiller, B., Queck, R., Kostner, B., and Bernhofer, C.: Comparison of surface energy exchange models with eddy flux data in forest and grassland ecosystems of Germany, Ecol Model, 188, 174-216, 10.1016/j.ecolmodel.2005.01.057, 2005.

Gettelman, A., and Fu, Q.: Observed and simulated upper-tropospheric water vapor feedback, J Climate, 21, 3282-3289, 10.1175/2007jcli2142.1, 2008.

Gilgen, H., Wild, M., and Ohmura, A.: Means and trends of shortwave irradiance at the surface estimated from global energy balance archive data, J Climate, 11, 2042-2061, 10.1175/1520-0442-11.8.2042, 1998.

Hartmann, D. L., Ramanathan, V., Berroir, A., and Hunt, G. E.: Earth radiation budget data and climate research, Rev Geophys, 24, 439-468, 10.1029/RG024i002p00439, 1986.

Hartmann, D. L., Tank, A. M. G. K., and Rusticucci, M.: Observation: Atmosphere and surface, IPCC, 1533 pp, 10.1017/CBO09781107415324, 2013.

Hegerl, G. C., and Zwiers, F. W.: Climate change 2007: Understanding and attributing climate change, Cambridge University Press, 1007 pp., 2007.

Hingray, B., Mezghani, A., and Buishand, T. A.: Development of probability distributions for regional climate change from uncertain global mean warming and an uncertain scaling relationship, Hydrol Earth Syst Sc, 11, 1097-1114, 2007.

Huang, J., Guan, X., and Ji, F.: Enhanced cold-season warming in semi-arid regions, Atmos. Chem. Phys., 12, 5391-5398, 10.5194/acp-12-5391-2012, 2012.

Jones, P. D., and Moberg, A.: Hemispheric and large-scale surface air temperature variations: An extensive revision and an update to 2001, J Climate, 16, 206-223, 10.1175/1520-0442(2003)016<0206:halssa>2.0.co;2, 2003.

Kalnay, E., and Cai, M.: Impact of urbanization and land-use change on climate, Nature, 423, 528-531, 10.1038/nature01675, 2003.

Karl, T. R., Kukla, G., Razuvayev, V. N., Changery, M. J., Quayle, R. G., Heim, R. R., Easterling, D. R., and Fu, C. B.: Global warming - evidence for asymmetric diurnal temperature-change, Geophys Res Lett, 18, 2253-2256, 10.1029/91gl02900, 1991.

Karoly, D. J., and Stott, P. A.: Anthropogenic warming of central England temperature, Atmos. Sci. Lett., 7, 81-85, 10.1002/asl.136, 2006.

Kukla, G., and Karl, T. R.: Nighttime warming and the greenhouse-effect, Environ Sci Technol, 27, 1468-1474, 10.1021/es00045a001, 1993.

Lauritsen, R. G., and Rogers, J. C.: US Diurnal Temperature Range Variability and Regional Causal Mechanisms, 1901-2002, J Climate, 25, 7216-7231, 10.1175/jcli-d-11-00429.1, 2012.

Li, B. F., Chen, Y. N., and Shi, X.: Why does the temperature rise faster in the arid region of northwest China?, J Geophys Res-Atmos, 117, 10.1029/2012jd017953, 2012.

Li, Q. X., Yang, S., Xu, W. H., Wang, X. L. L., Jones, P., Parker, D., Zhou, L. M., Feng, Y., and Gao, Y.: China experiencing the recent warming hiatus, Geophys Res Lett, 42, 889-898, 10.1002/2014gl062773, 2015.

Liang, F., and Xia, X. A.: Long-term trends in solar radiation and the associated climatic factors over China for 1961-2000, Ann Geophys, 23, 2425-2432, 2005.

Liepert, B. G.: Observed reductions of surface solar radiation at sites in the United States and worldwide from 1961 to 1990, Geophys Res Lett, 29, 10.1029/2002gl014910, 2002.

Lim, Y. K., Cai, M., Kalnay, E., and Zhou, L. M.: Observational evidence of sensitivity of surface climate changes to land types and urbanization, Geophys Res Lett, 32, 4, 10.1029/2005gl024267, 2005.

Liu, B. H., Xu, M., Henderson, M., Qi, Y., and Li, Y. Q.: Taking China's temperature: Daily range, warming trends, and regional variations, 1955-2000, J Climate, 17, 4453-4462, 10.1175/3230.1, 2004.

Liu, J. Y., Liu, M. L., Tian, H. Q., Zhuang, D. F., Zhang, Z. X., Zhang, W., Tang, X. M., and Deng, X. Z.: Spatial and temporal patterns of China's cropland during 1990-2000: An analysis based on Landsat TM data, Remote Sens Environ, 98, 442-456, 10.1016/j.rse.2005.08.012, 2005.

Mahlstein, I., and Knutti, R.: Regional climate change patterns identified by cluster analysis, Clim Dynam, 35, 587-600, 10.1007/s00382-009-0654-0, 2010.

Makowski, K., Jaeger, E. B., Chiacchio, M., Wild, M., Ewen, T., and Ohmura, A.: On the relationship between diurnal temperature range and surface solar radiation in Europe, J Geophys Res-Atmos, 114, 16, 10.1029/2008jd011104, 2009.

Manara, V., Beltrano, M. C., Brunetti, M., Maugeri, M., Sanchez-Lorenzo, A., Simolo, C., and Sorrenti, S.: Sunshine duration variability and trends in Italy from homogenized instrumental time series (1936-2013), J Geophys Res-Atmos, 120, 3622-3641, 10.1002/2014jd022560, 2015.

Mariotti, L., Coppola, E., Sylla, M. B., Giorgi, F., and Piani, C.: Regional climate model simulation of projected 21st century climate change over an all-Africa domain: Comparison analysis of nested and driving model results, J Geophys Res-Atmos, 116, 10.1029/2010jd015068, 2011.

Menon, S., Hansen, J., Nazarenko, L., and Luo, Y. F.: Climate effects of black carbon aerosols in China and India, Science, 297, 2250-2253, 10.1126/science.1075159, 2002.

Ohmura, A.: Observed long-term variations of solar irradiance at the earth's surface, Space Sci Rev, 125, 111-128, 10.1007/s11214-006-9050-9, 2006.

Peng, S. S., Piao, S. L., Zeng, Z. Z., Ciais, P., Zhou, L. M., Li, L. Z. X., Myneni, R. B., Yin, Y., and Zeng, H.: Afforestation in China cools local land surface temperature, P Natl Acad Sci USA, 111, 2915-2919, 10.1073/pnas.1315126111, 2014.

Ren, G., Xu, M., Chu, Z., Guo, J., Li, Q., Liu, X., and Wang, Y.: Changes of Surface Air Temperature in China During 1951-2004, Climatic and environmental research, 10, 717-727, 2005.

Roy, I., and Haigh, J. D.: The influence of solar variability and the quasi-biennial oscillation on lower atmospheric temperatures and sea level pressure, Atmos. Chem. Phys., 11, 11679-11687, 10.5194/acp-11-11679-2011, 2011.

Sanchez-Lorenzo, A., and Wild, M.: Decadal variations in estimated surface solar radiation over Switzerland since the late 19th century, Atmos. Chem. Phys., 12, 8635-8644, 10.5194/acp-12-8635-2012, 2012.

Seneviratne, S. I., Corti, T., Davin, E. L., Hirschi, M., Jaeger, E. B., Lehner, I., Orlowsky, B., and Teuling, A. J.: Investigating soil moisture-climate interactions in a changing climate: A review, Earth-sci Rev, 99, 125-161, 10.1016/j.earscirev.2010.02.004, 2010.

Shen, D. J., and Varis, O.: Climate change in China, Ambio, 30, 381-383, 10.1639/0044-7447(2001)030[0381:ccic]2.0.co;2, 2001.

Shen, M. G., Piao, S. L., Jeong, S. J., Zhou, L. M., Zeng, Z. Z., Ciais, P., Chen, D. L., Huang, M. T., Jin, C. S., Li, L. Z. X., Li, Y., Myneni, R. B., Yang, K., Zhang, G. X., Zhang, Y. J., and Yao, T. D.: Evaporative cooling over the Tibetan Plateau induced by vegetation growth, P Natl Acad Sci USA, 112, 9299-9304, 10.1073/pnas.1504418112, 2015.

Shen, X. J., Liu, B. H., Li, G. D., Wu, Z. F., Jin, Y. H., Yu, P. J., and Zhou, D. W.: Spatiotemporal change of diurnal temperature range and its relationship with sunshine duration and precipitation in China, J Geophys Res-Atmos, 119, 13163-13179, 10.1002/2014jd022326, 2014.

Shi, G. Y., Hayasaka, T., Ohmura, A., Chen, Z. H., Wang, B., Zhao, J. Q., Che, H. Z., and Xu, L.: Data quality assessment and the long-term trend of ground solar radiation in China, J. Appl. Meteorol. Clim., 47, 1006-1016, 10.1175/2007jamc1493.1, 2008.

Stanhill, G., and Cohen, S.: Global dimming: a review of the evidence for a widespread and significant reduction in global radiation with discussion of its probable causes and possible agricultural consequences, Agr Forest Meteorol, 107, 255-278, 10.1016/s0168-

1923(00)00241-0, 2001.

Sun, Y., Zhang, X. B., Ren, G. Y., Zwiers, F. W., and Hu, T.: Contribution of urbanization to warming in China, Nature Climate Change, 6, 706-+, 10.1038/nclimate2956, 2016.

Tang, W. J., Yang, K., Qin, J., Cheng, C. C. K., and He, J.: Solar radiation trend across China in recent decades: a revisit with quality-controlled data, Atmos. Chem. Phys., 11, 393-406, 10.5194/acp-11-393-2011, 2011.

Taylor, J. R., Randel, W. J., and Jensen, E. J.: Cirrus cloud-temperature interactions in the tropical tropopause layer: a case study, Atmos. Chem. Phys., 11, 10085-10095, 10.5194/acp-11-10085-2011, 2011.

Tebaldi, C., Smith, R. L., Nychka, D., and Mearns, L. O.: Quantifying uncertainty in projections of regional climate change: A Bayesian approach (vol 18, pg 1524, 2005), J Climate, 18, 3405-3405, 10.1175/JCLI9001.1a, 2005.

Vautard, R., Yiou, P., and van Oldenborgh, G. J.: Decline of fog, mist and haze in Europe over the past 30 years, Nat Geosci, 2, 115-119, 10.1038/ngeo414, 2009.

Vose, R. S., Easterling, D. R., and Gleason, B.: Maximum and minimum temperature trends for the globe: An update through 2004, Geophys Res Lett, 32, 10.1029/2005gl024379, 2005.

Wallace, J. M., Fu, Q., Smoliak, B. V., Lin, P., and Johanson, C. M.: Simulated versus observed patterns of warming over the extratropical Northern Hemisphere continents during the cold season, P Natl Acad Sci USA, 109, 14337-14342, 10.1073/pnas.1204875109, 2012.

Wang, K., and Dickinson, R. E.: Global atmospheric downward longwave radiation at the surface from ground-based observations, satellite retrievals, and reanalyses, Rev Geophys, 51, 150-185, 10.1002/rog.20009, 2013a.

Wang, K., and Dickinson, R. E.: Contribution of solar radiation to decadal temperature variability over land, P Natl Acad Sci USA, 110, 14877-14882, 10.1073/pnas.1311433110, 2013b.

Wang, K. C., Li, Z. Q., and Cribb, M.: Estimation of evaporative fraction from a combination of day and night land surface temperatures and NDVI: A new method to determine the Priestley-Taylor parameter, Remote Sens Environ, 102, 293-305, 10.1016/j.rse.2006.02.007, 2006.

Wang, K. C., and Dickinson, R. E.: A review of global terrestrial evapotranspiration: Observation, modeling, climatology, and climatic variability, Rev Geophys, 50, 10.1029/2011rg000373, 2012.

Wang, K. C., Dickinson, R. E., Wild, M., and Liang, S.: Atmospheric impacts on climatic variability of surface incident solar radiation, Atmos. Chem. Phys., 12, 9581-9592, 10.5194/acp-12-9581-2012, 2012.

Wang, K. C.: Measurement Biases Explain Discrepancies between the Observed and Simulated Decadal Variability of Surface Incident Solar Radiation, Sci. Rep, 4, 10.1038/srep06144, 2014.

Wang, K. C., Ma, Q., Li, Z. J., and Wang, J. K.: Decadal variability of surface incident solar radiation over China: Observations, satellite retrievals, and reanalyses, J Geophys Res-Atmos, 120, 6500-6514, 10.1002/2015jd023420, 2015a.

Wang, K. C., and Zhou, C. L. E.: Regional Contrasts of the Warming Rate over Land Significantly Depend on the Calculation Methods of Mean Air Temperature, Sci. Rep, 5, 10.1038/srep12324, 2015.

Wang, X., Wang, K., and Su, L.: Contribution of Atmospheric Diffusion Conditions to the Recent Improvement in Air Quality in China, Sci. Rep, 6, 36404, 10.1038/srep36404, 2016.

Wang, Y. J., Chen, X. Y., and Yan, F.: Spatial and temporal variations of annual precipitation during 1960-2010 in China, Quatern Int, 380, 5-13, 10.1016/j.quaint.2014.12.047, 2015b.

Weng, Q. H., Lu, D. S., and Schubring, J.: Estimation of land surface temperature-vegetation abundance relationship for urban heat island studies, Remote Sens Environ, 89, 467-483, 10.1016/j.rse.2003.11.005, 2004.

Wild, M., Ohmura, A., and Makowski, K.: Impact of global dimming and brightening on global warming, Geophys Res Lett, 34, 10.1029/2006gl028031, 2007.

Wild, M.: Enlightening global dimming and brightening, B Am Meteorol Soc, 93, 27-37, 10.1175/bams-d-11-00074.1, 2012.

Xia, X.: A closer looking at dimming and brightening in China during 1961-2005, Ann Geophys, 28, 1121-1132, 10.5194/angeo-28-1121-2010, 2010.

Yang, K., Koike, T., and Ye, B. S.: Improving estimation of hourly, daily, and monthly solar radiation by importing global data sets, Agr Forest Meteorol, 137, 43-55, 10.1016/j.agrformet.2006.02.001, 2006.

Yin, Z., Wang, H., and Chen, H.: Understanding Severe Winter Haze Pollution in the North-Central North China Plain in 2014, Atmos. Chem. Phys., 2016, 1-27, 10.5194/acp-2016-641, 2016.

You, Q. L., Min, J. Z., Jiao, Y., Sillanpaa, M., and Kang, S. C.: Observed trend of diurnal temperature range in the Tibetan Plateau in recent decades, Int J Climatol, 36, 2633-2643, 10.1002/joc.4517, 2016.

Zhai, P. M., Zhang, X. B., Wan, H., and Pan, X. H.: Trends in total precipitation and frequency of daily precipitation extremes over China, J Climate, 18, 1096-1108, 10.1175/jcli-3318.1, 2005.

Zhang, X., Sun, Y., Mao, W., Liu, Y., and Ren, Y.: Regional Response of Temperature Change in the Arid Regions of China to Global Warming, Arid Zone Research, 27, 592-599, 2010.

Zhang, Z. X., Li, N., Wang, X., Liu, F., and Yang, L. P.: A Comparative Study of Urban Expansion in Beijing, Tianjin and Tangshan from the 1970s to 2013, Remote. Sen., 8, 22, 10.3390/rs8060496, 2016.

Zhou, C. L., and Wang, K. C.: Coldest Temperature Extreme Monotonically Increased and Hottest Extreme Oscillated over Northern Hemisphere Land during Last 114 Years, Sci. Rep, 6, 10.1038/srep25721, 2016.

Zhou, L. M., Dickinson, R. E., Tian, Y. H., Fang, J. Y., Li, Q. X., Kaufmann, R. K., Tucker, C. J., and Myneni, R. B.: Evidence for a significant urbanization effect on climate in China, P Natl Acad Sci USA, 101, 9540-9544, 10.1073/pnas.0400357101, 2004.

Zhou, L. M., Dickinson, R. E., Tian, Y. H., Vose, R. S., and Dai, Y. J.: Impact of vegetation removal and soil aridation on diurnal temperature range in a semiarid region: Application to the Sahel, P Natl Acad Sci USA, 104, 17937-17942, 10.1073/pnas.0700290104, 2007.

Zhou, L. M., Dai, A., Dai, Y. J., Vose, R., Zou, C. Z., Tian, Y. H., and Chen, H. S.: Spatial dependence of diurnal temperature range trends on precipitation from 1950 to 2004, Clim Dynam, 32, 429-440, 10.1007/s00382-008-0387-5, 2009.

Zhou, L. M., Dickinson, R. E., Dai, A. G., and Dirmeyer, P.: Detection and attribution of anthropogenic forcing to diurnal temperature range changes from 1950 to 1999: comparing multi-model simulations with observations, Clim Dynam, 35, 1289-1307, 10.1007/s00382-009-0644-2, 2010.

Zhou, Y. Q., and Ren, G. Y.: Change in extreme temperature event frequency over mainland China, 1961-2008, Climate Res, 50, 125-139, 10.3354/cr01053, 2011.

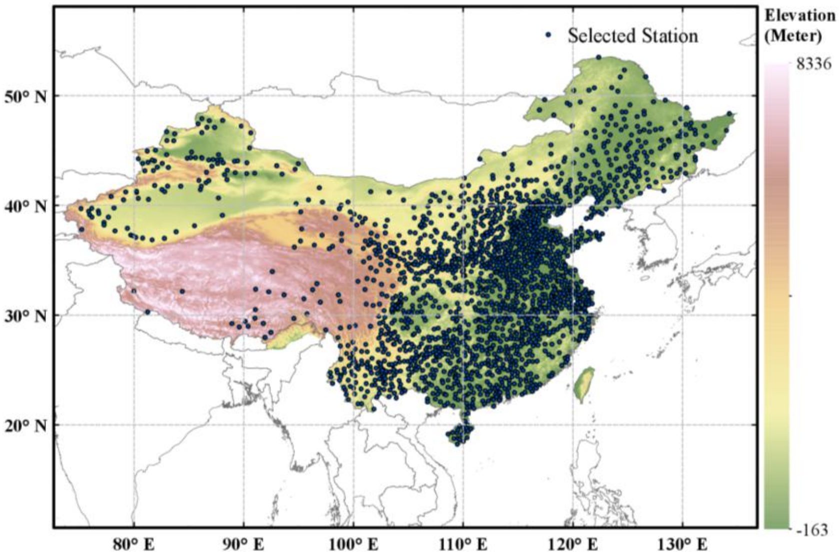

Figure~~.~~ 1. Elevation maps of m~~M~~ainland China and~~ the~~ spatial distribution of the 1977 meteorological stations used in this study. ~~Although the datasets have good spatial coverage, the spatial heterogeneity of the station density between West and East China is significant. To reduce the impact of spatial heterogeneity on the statistical results, we used the area-weight average method to analyze the trends or variations when taking China as a whole.~~ The datasets ~~are~~ were provided by China's National Meteorological Information ~~Center~~ Centre (You et al., 2016) (**http://data.cma.gov.cn/data**).

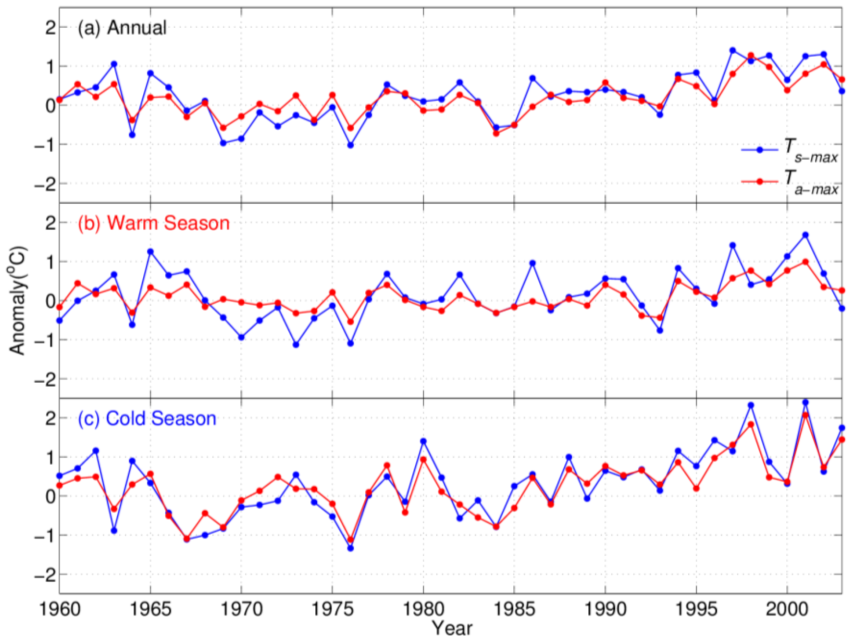

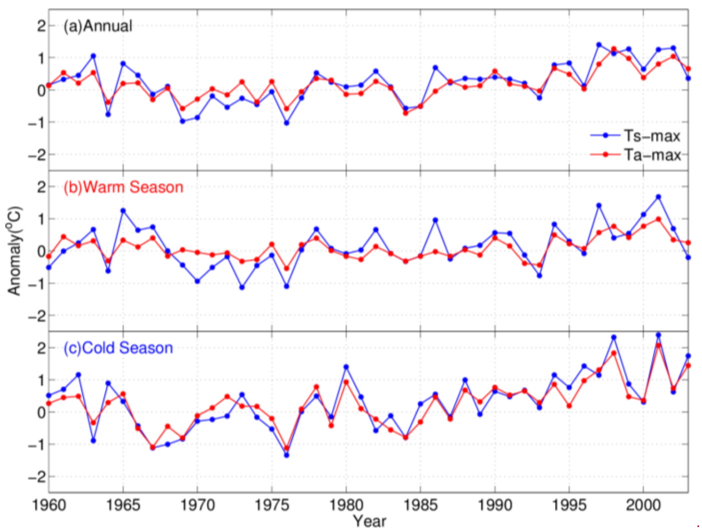

Figures~~.~~ 2. National mean yearly anomalies of daily maximum land surface temperature

($T_{s\text{-}max}$, blue line) and daily maximum air temperature ($T_{a\text{-}max}$, red line) for the annual (a), warm (b), and cold (c) seasonal scales for the reference period from 1961 to 1990.~~National mean yearly anomalies of $T_{s\text{-}max}$ (blue line) and $T_{a\text{-}max}$ (red line) on annual (a), warm (b), and cold (c) seasonal scales for the reference period of 1961–1990. The trends and fluctuations of the annual anomalies of $T_{s\text{-}max}$ and $T_{a\text{-}max}$ are similar to each other. The similarity between them is greater in the cold seasons than in the warm seasons, probably because of seasonal differences in precipitation, SSR, and convection intensity.~~

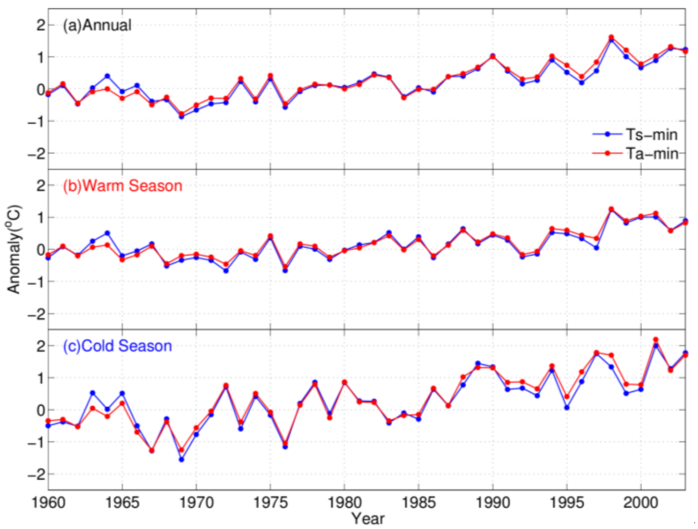

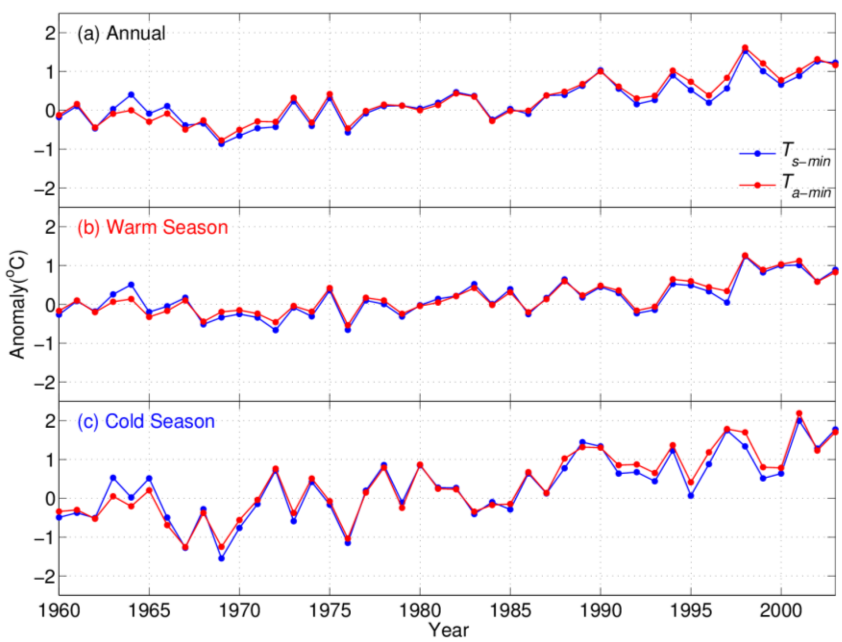

Fig~~s.~~ure 3. National mean yearly anomalies of daily minimum land surface temperature (T_{s-min}, blue line) and daily minimum air temperature (T_{a-min}, red line) ~~T_{s-min} (blue line) and T_{a-min} (red line) on~~for the annual (a), warm (b), and cold (c) seasonal scales for the reference period 1961-1990. ~~The trends and fluctuations in the annual anomalies of T_{s-min} and T_{a-min} are extremely similar to each other. Compared to the similarity in maximum temperatures (see Fig. 3), the similarity between T_{s-min} and T_{a-min} is greater and has no obvious seasonal differences. This is consistent with the near-surface atmosphere being more stable during the night. T_{s-min} and T_{a-min} have little relationship with the precipitation and SSR on the seasonal scale.~~

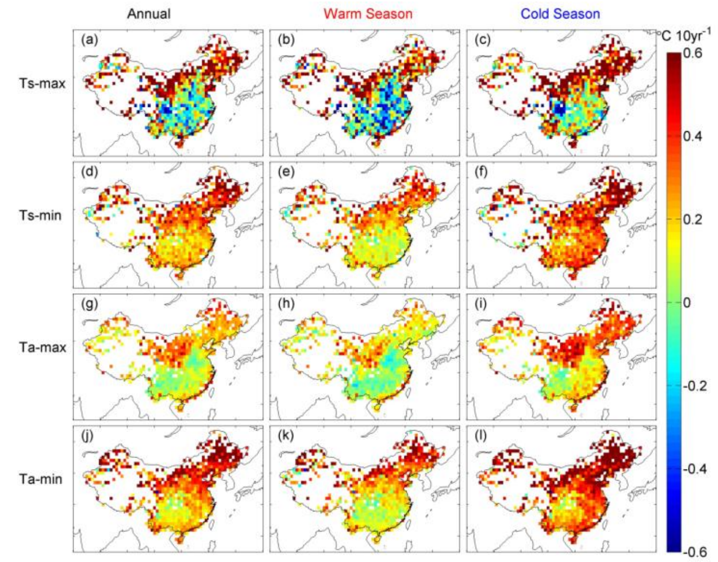

Annual
Warm Season
Cold Season
°C 10yr-1
Ts-max
Ts-min
Ta-max
Ta-min
(a)
(b)
(c)
(d)
(e)
(f)
(g)
(h)
(i)
(j)
(k)
(l)
0.6
0.4
0.2
0
-0.2
-0.4
-0.6

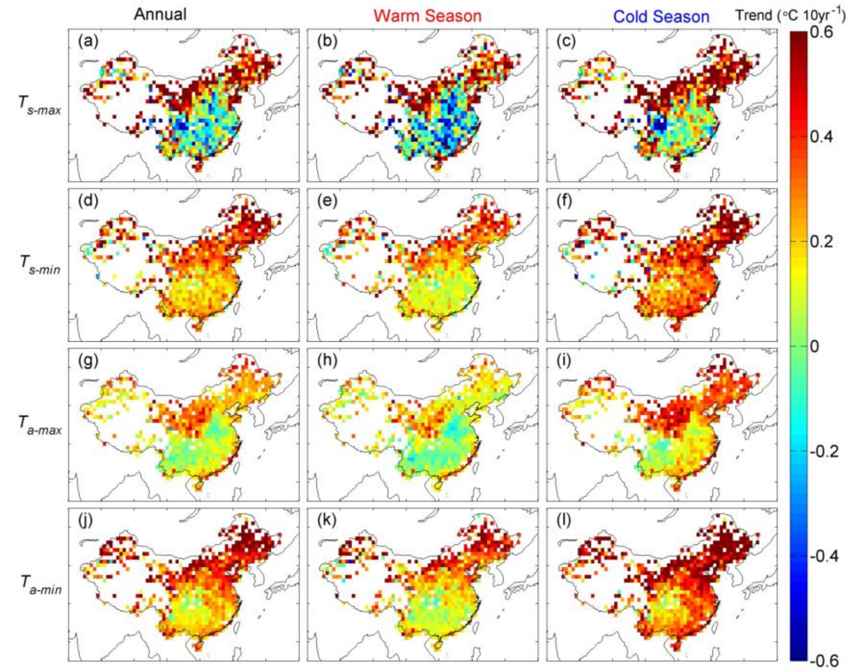

Annual
Warm Season
Cold Season
Trend (°C 10yr-1)
Ts-max
Ts-min
Ta-max
Ta-min
(a)
(b)
(c)
(d)
(e)
(f)
(g)
(h)
(i)
(j)
(k)
(l)
0.6
0.4
0.2
0
-0.2
-0.4
-0.6

Figure~~s.~~ 4. Maps of the trends of the monthly anomalies for daily maximum land surface temperature ($T_{s\text{-}max}$, a–c), daily minimum land surface temperature ($T_{s\text{-}min}$, d–f), daily maximum air temperature ($T_{a\text{-}max}$, g–i), and daily minimum air temperature ($T_{a\text{-}min}$, j–l) for the annual, warm (May–October), and cold (November–next April) seasonal scales. All trends reported in these figures were calculated using a linear regression based on the least square method.~~T~~$\cancel{T_{s\text{-}max}}$ ~~(a–c),~~ $\cancel{T_{s\text{-}min}}$ ~~(d–f),~~ $\cancel{T_{a\text{-}max}}$ ~~(g–i), and~~ $\cancel{T_{a\text{-}min}}$ ~~(j–l) on annual, warm (May–October), and cold (November–next April) seasonal scales. For the maximum temperatures (~~$\cancel{T_{s\text{-}max}}$ ~~and~~ $\cancel{T_{a\text{-}max}}$~~), the warming rates on the North China Plain and in South China are significantly lower than in other regions. For~~ $\cancel{T_{s\text{-}min}}$ ~~and~~ $\cancel{T_{a\text{-}min}}$~~, the warming rates are the highest in North China and generally diminish from north to south. The warming rates of the temperatures are higher in the cold seasons than in the warm seasons, whereas the spatial difference in the warming rates of the temperatures is higher in the warm seasons than in the cold seasons.~~

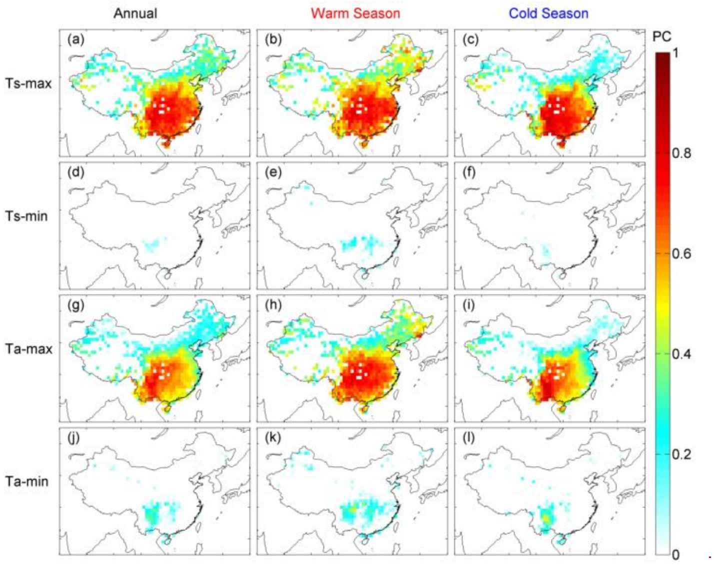

~~Figs. 5. Maps of the partial correlation coefficients (PCs) between the surface solar radiation (SSR) and the temperatures on annual, warm, and cold seasonal scales. The PCs are the linear partial correlation coefficients calculated based on the monthly anomalies of the SSR and temperatures, taking the precipitation as a control variable. Both $T_{s\text{-}max}$ and $T_{a\text{-}max}$ have a significant correlation with SSR. The correlations between $T_{s\text{-}max}$ and SSR in 99.7% of the stations are statistically significant at the 1% level on the seasonal scale. The correlations between $T_{a\text{-}max}$ and SSR in 95.4% of the stations are statistically significant at the 1% level. Both $T_{s\text{-}min}$ and $T_{a\text{-}min}$ have no significant correlation with SSR.~~

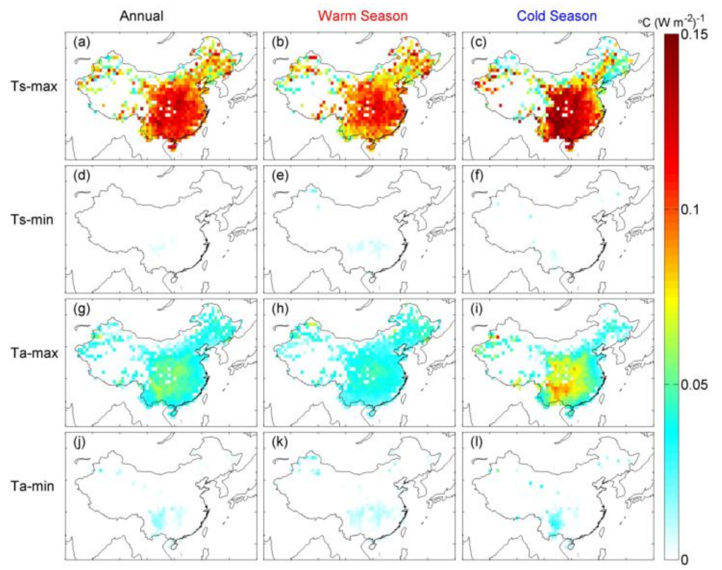

~~Figs. 6. Maps of the sensitivity of the temperatures to the surface solar radiation (SSR) variation on annual, warm, and cold seasonal scales. The sensitivity of T_{s-max} to SSR is largest because solar radiation directly heats the land surface during the day. After land surface warming, part of the energy from the SSR will heat the near-surface air via the sensitive heat flux; therefore, T_{a-max} also has significant sensitivity to SSR. T_{s-min} and T_{a-min} primarily depend on the atmospheric longwave radiation during the night; therefore, they are not significantly sensitive to SSR. In addition, T_{s-max} and T_{a-max}'s sensitivities to SSR are higher in the cold seasons than in the warm seasons, probably because of seasonal differences in the soil moisture.~~

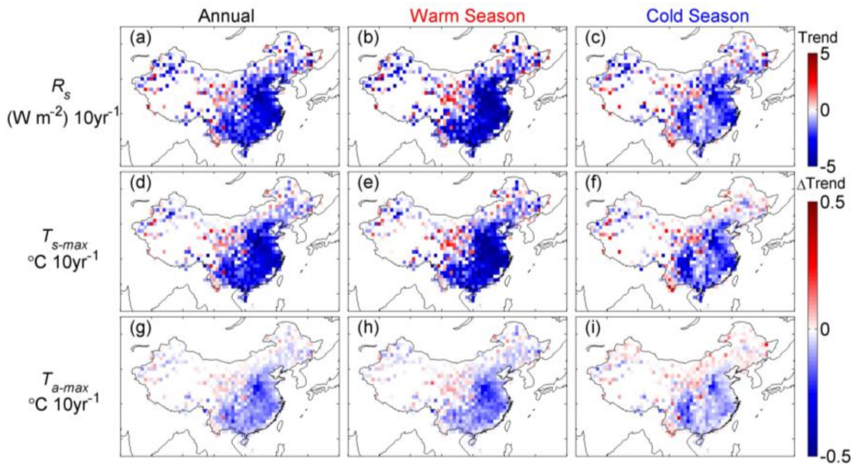

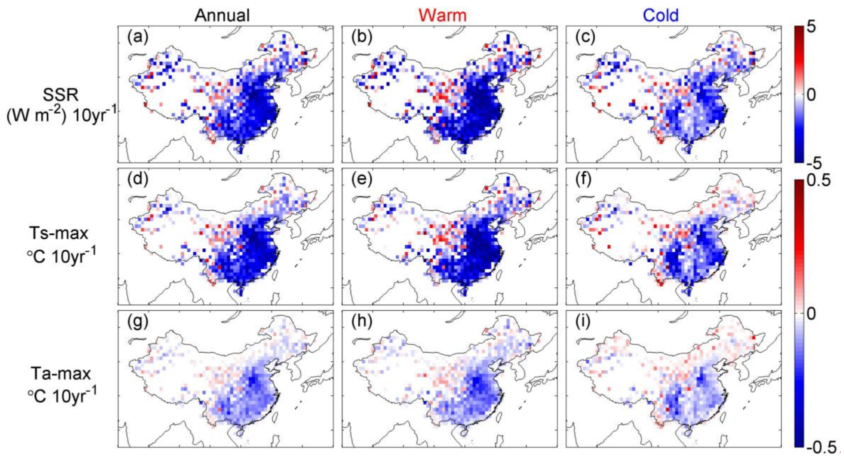

Fig~~s.~~ure ~~7~~5. Maps of the trends in surface solar radiation (R_s, a–c) and its effect on the warming rates of daily maximum land surface temperature ($T_{s\text{-}max}$, d–f) and daily maximum air temperature ($T_{a\text{-}max}$, g–i). The first line (a-c) is the trend of R_s from 1960-2003; the second line (d-f) and the third line (g-i) are the trend changes caused by secular variations of R_s on T_{s-max} and T_{a-max}. Eq (1) was used to strip away the effect of R_s on temperatures, and we calculated the trend difference (ΔTrend, d-i) between the time series of temperatures before and after adjusting for the effect of R_s. Finally, the effect of R_s on the trends of T_{s-max}/T_{a-max} was quantified and analyzed (section 3.2.1).~~Maps of the trends in surface solar radiation (SSR) (a–c) and its impact on the warming rates of~~ ~~T_{s-max} (d–f) and T_{a-max} (g–i).~~

~~The decreasing rate of SSR is highest on the North China Plain and in South China. The reduction of SSR resulted in the decreasing trends of~~ ~~T_{s-max} and T_{a-max} on the North China Plain and in South China, which is consistent with the lower warming rates of~~ ~~T_{s-max} and T_{a-max} in the North China Plain and South China than in other regions (see Figs. 4). The decreasing rate of SSR is higher in the warm seasons than in the cold seasons, which results in the spatial difference between the North China Plain and the South China Plain and other regions being more significant in the warm seasons than in the cold seasons.~~

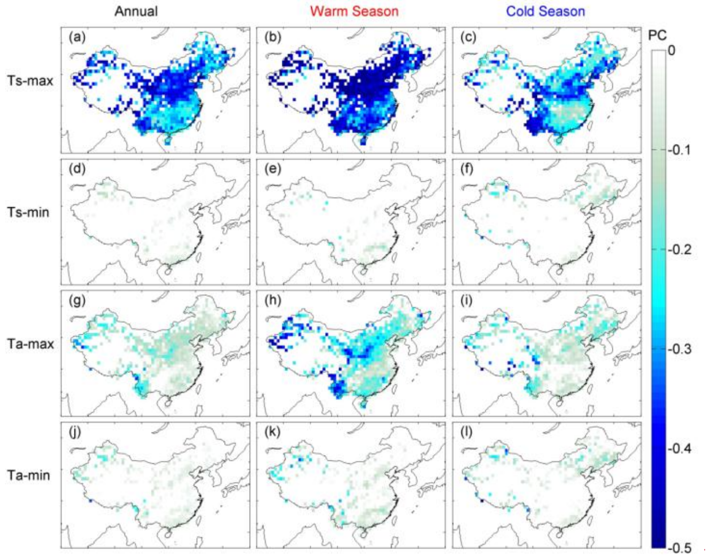

~~Figs. 8. The partial correlation coefficients (PCs) between the precipitation and the temperatures on annual, warm, and cold seasonal scales. The PCs are the linear partial correlation coefficients calculated based on the monthly anomalies of the precipitation and temperatures, taking SSR as a control variable. $T_{s\text{-}max}$ has a significant correlation with precipitation. The correlations between $T_{s\text{-}max}$ and precipitation in 99.3% of the stations are statistically significant at the 1% level. The correlation between $T_{a\text{-}max}$ and precipitation is significant at the 1% level in some regions (for 35.1% of China). Both $T_{s\text{-}min}$ and $T_{a\text{-}min}$ have no significant correlation with SSR.~~

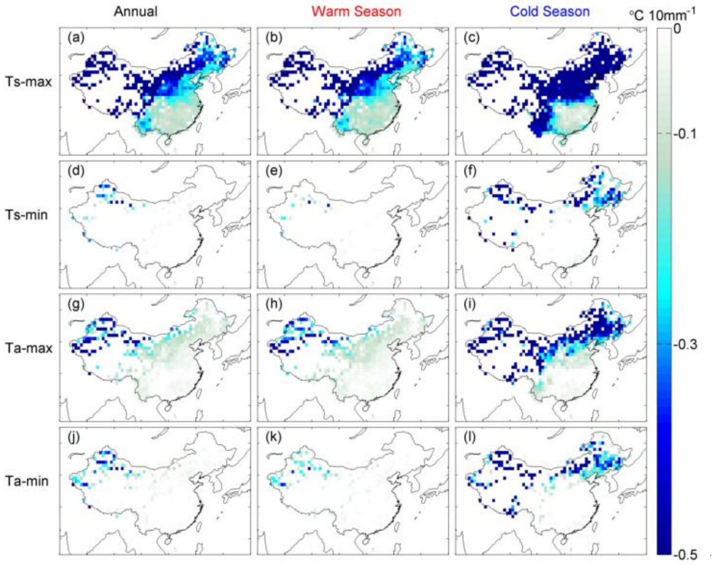

~~Figs. 9. Maps of the sensitivity of the temperatures to precipitation variation on annual, warm, and cold seasonal scales. The sensitivity of T_{s-max} to precipitation is highest because the soil thermal capacity and evaporative cooling effect of the land surface depends on soil moisture resulting from precipitation. In addition, the precipitation determines the fraction of SSR generating sensitive heat flux by altering the soil moisture and has an important effect on T_{s-max} and T_{a-max}. In arid and semi-arid areas, the soil moisture is far less than the potential evapotranspiration, and precipitation has a greater effect on evapotranspiration and further affects T_{s-max} and T_{a-max}. Therefore, sensitivities of T_{s-max} and T_{a-max} are higher in arid and semiarid areas than in others.~~

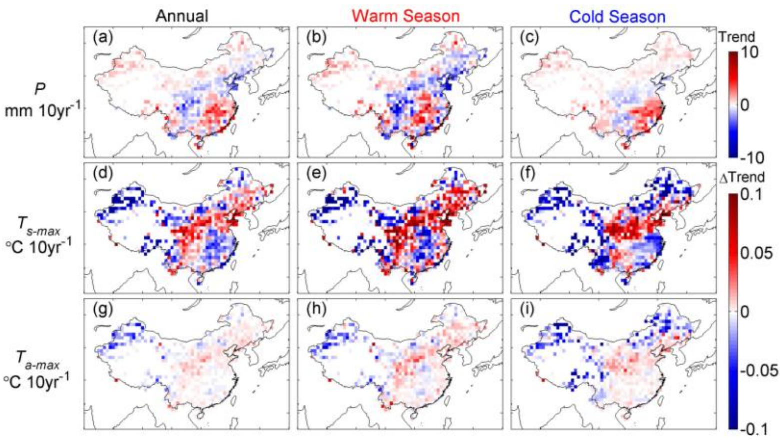

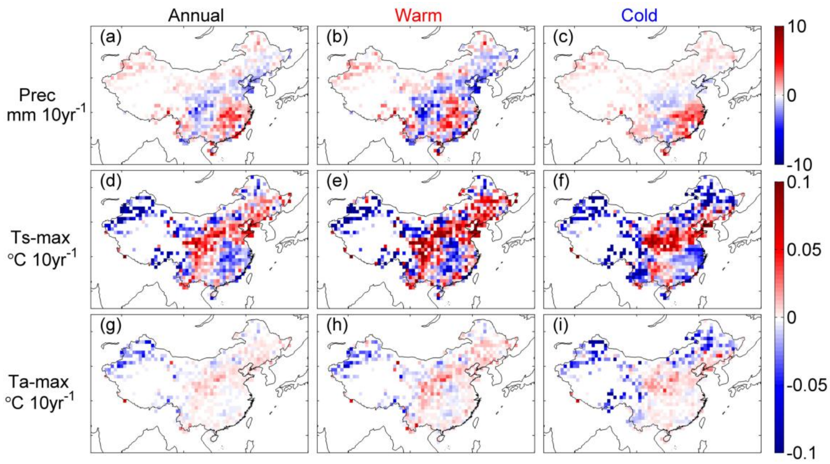

Figures~~.~~ ~~10~~6. Maps of the trends in precipitation (*P*) (a–c) and their effect on the warming rates for daily maximum land surface temperature ($T_{s\text{-}max}$, d–f) and daily maximum air temperature ($T_{a\text{-}max}$, g–i). The first line (a-c) is the trend of *P* during 1960-2003; the second line (d-f) and the third line (g-i) are the trend changes caused by secular variations of *P* on $T_{s\text{-}max}$ and $T_{a\text{-}max}$. We used Eq (1) to remove the effects of *P* on the temperatures, then calculated the trend difference (ΔTrend, d-i) between the time series of temperatures before and after adjusting for the effect of *P*. Finally, the effect of *P* on the trends of T_{s-max}/T_{a-max} was quantified and analyzed (section 3.2.2). ~~Maps of the trends in precipitation (Prec) (a–c) and their impact on the warming rates for T_{s-max} (d–f) and T_{a-max} (g–i).~~

~~Globally, precipitation in China has a slight increasing trend (0.112 mm 10yr^{-1}) during the period of 1960–2003 (a). Precipitation in Northwestern and Southeastern China had an increasing trend, whereas precipitation in the North China Plain, the Sichuan Basin, and parts of Northeastern China had a decreasing trend. The variation in precipitation in the warm seasons is more significant than in the cold seasons. For T_{s-max} and T_{s-max}, the reduction in precipitation aggravated the warming trend in the North China Plain, the Sichuan Basin, and parts of Northeastern China, while the increase in precipitation primarily slowed the warming trend in Northwestern China and on the Mongolian Plateau. However, the impact of precipitation on T_{s-max} and T_{a-max} is far smaller than that of SSR.~~

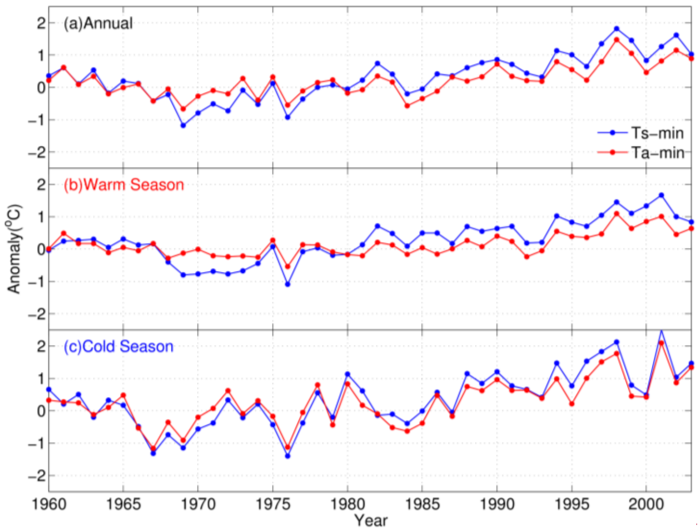

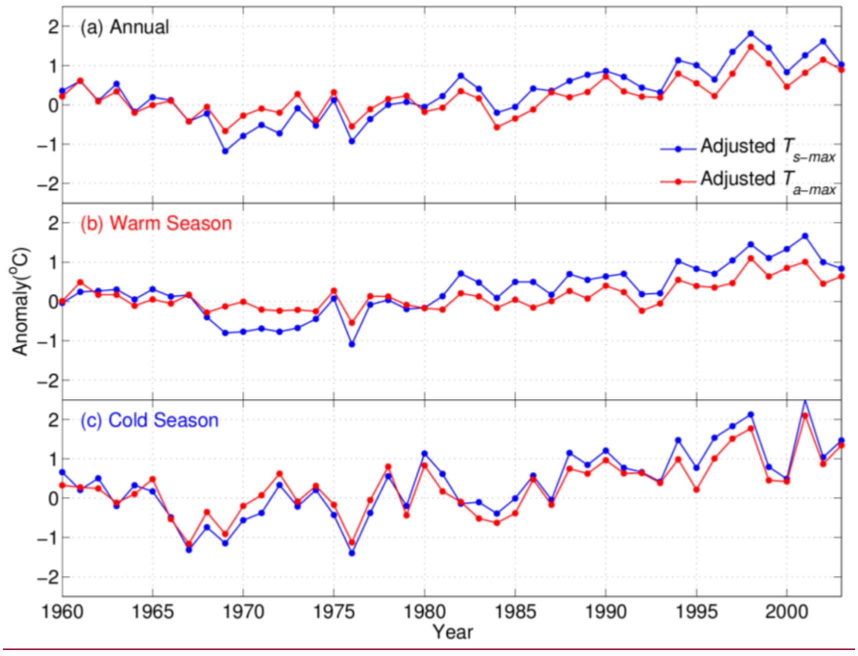

Figures~~.~~ ~~11~~7. ~~After adjusting for the impact of SSR and precipitation, r~~Regional~~ly~~

average anomalies of daily maximum land surface temperature ($T_{s\text{-}max}$, blue line) and daily maximum air temperature ($T_{a\text{-}max}$, red line) for the annual (a), warm (b), and cold (c) seasonal scales for the reference period from 1961 to 1990. We used Eq (1) to simultaneously adjust for the effects of surface solar radiation (R_s) and precipitation (P) on $T_{s\text{-}max}/T_{a\text{-}max}$ and then analyzed the changes in the interannual variation of $T_{s\text{-}max}/T_{a\text{-}max}$ (section 3.3). ~~$T_{s\text{-}max}$ (blue line) and $T_{a\text{-}max}$ (red line) on annual (a), warm (b), and cold (c) seasonal scales for the reference period of 1961-1990. After adjustments, the trends and fluctuations of $T_{s\text{-}max}$ and $T_{a\text{-}max}$ changed significantly, especially in the warm seasons. The fluctuation of $T_{s\text{-}max}$ remains similar to that of $T_{a\text{-}max}$, whereas the amount of the increase in the warming rate of $T_{s\text{-}max}$ (0.146 °C $10yr^{-1}$) is higher than that of $T_{a\text{-}max}$ (0.055 °C $10yr^{-1}$) because $T_{s\text{-}max}$ is more sensitive to the variation of SSR. In addition, this difference in the amount of the increase primarily occurred in the warm seasons, which is consistent with the greater reduction of SSR in the warm seasons (see Figs. 7a-c).~~

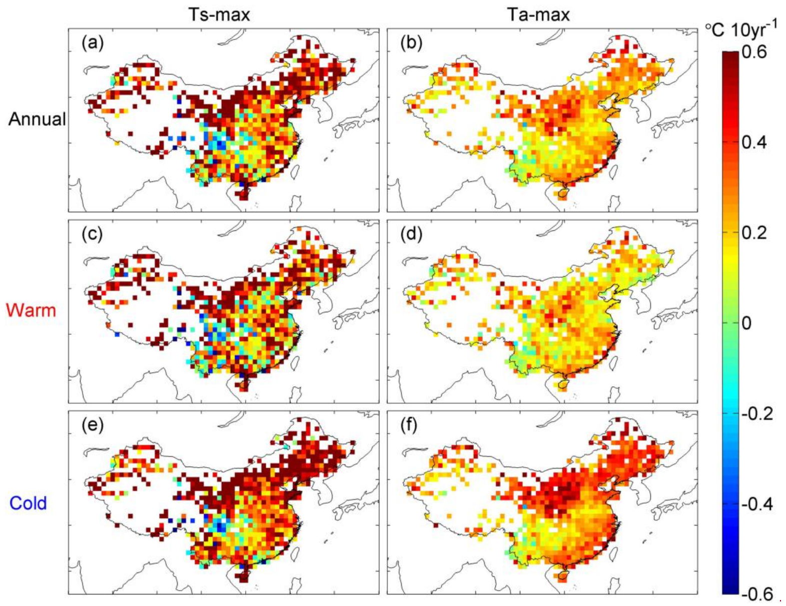
Ts-max
Ta-max
°C 10yr^{-1}
(a)
(b)
Annual
(c)
(d)
Warm
(e)
(f)
Cold
0.6
0.4
0.2
0
-0.2
-0.4
-0.6

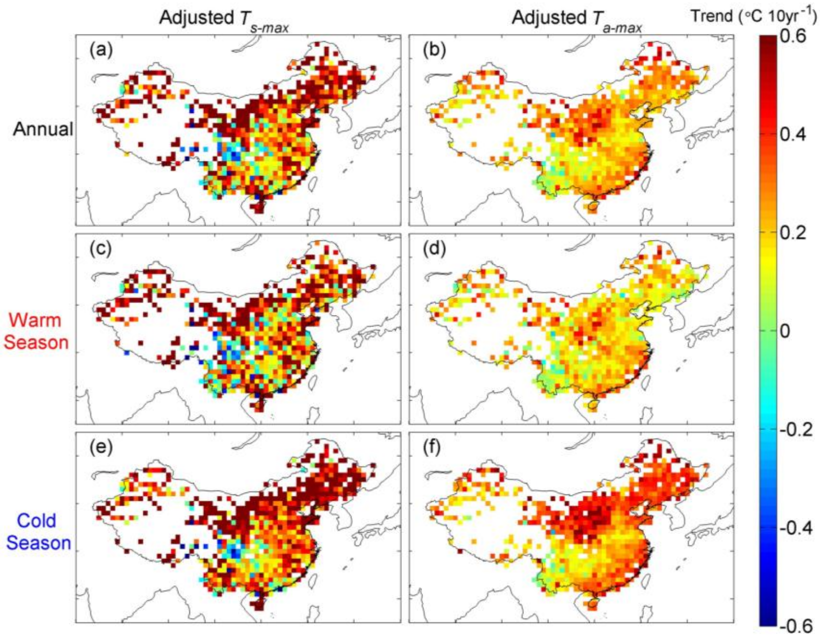
Adjusted $T_{s\text{-}max}$
Adjusted $T_{a\text{-}max}$
Trend (°C 10yr^{-1})
(a)
(b)
Annual
(c)
(d)
Warm Season
(e)
(f)
Cold Season
0.6
0.4
0.2
0
-0.2
-0.4
-0.6

Figure 8. Maps of the trends of the monthly anomalies for the daily maximum land surface temperature ($T_{s\text{-}max}$, a, c, e) and daily maximum air temperature ($T_{a\text{-}max}$, b, d, f) for the annual, warm, and cold seasonal scales after adjusting for the effects of surface solar radiation (R_s) and precipitation (P). We used Eq (1) to simultaneously adjust the effects of R_s and P on $T_{s\text{-}max}/T_{a\text{-}max}$ and then analyzed the changes in the secular trends of $T_{s\text{-}max}/T_{a\text{-}max}$ (section 3.3).~~Figs. 12. After correcting for the impact of solar radiation and precipitation, maps of the trends of the monthly anomalies for~~ ~~$T_{s\text{-}max}$~~ ~~(a, c, e) and~~ ~~$T_{a\text{-}max}$~~ ~~(b, d, f) on the annual, warm, and cold seasonal scales. After correcting for the impact of SSR and precipitation using multiple linear regression (see the Method Section), the warming rates of~~ ~~$T_{s\text{-}max}$~~ ~~and~~ ~~$T_{a\text{-}max}$~~ ~~in the North China Plain and South China are enhanced significantly, and the difference between them and other regions of China is clearly reduced. The difference between Figs. 4 and Figs. 12 indicates that the impact of SSR and precipitation is an important cause of the spatial heterogeneity of the warming rates in~~ ~~$T_{s\text{-}max}$~~ ~~and~~ ~~$T_{a\text{-}max}$.~~ ~~Combined with Figs. 7, we find that the impact of SSR plays a primary role in generating this spatial difference.~~

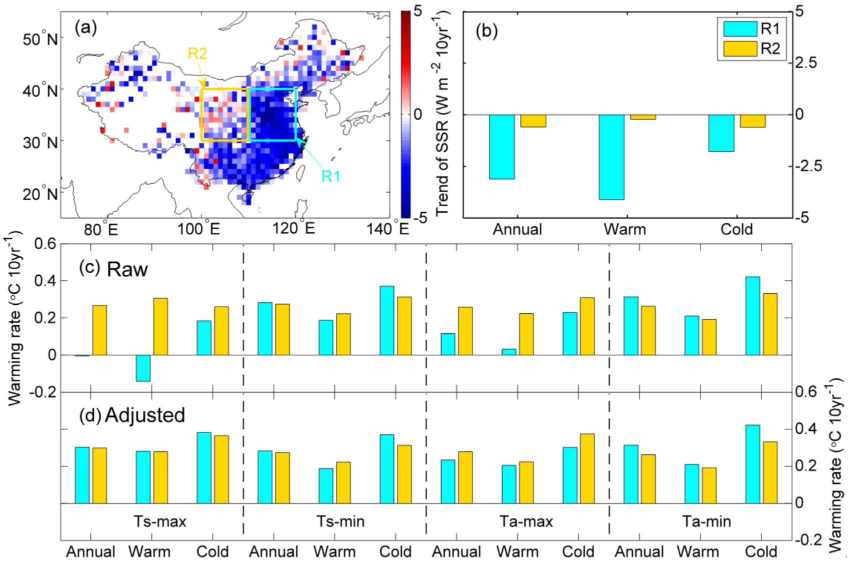

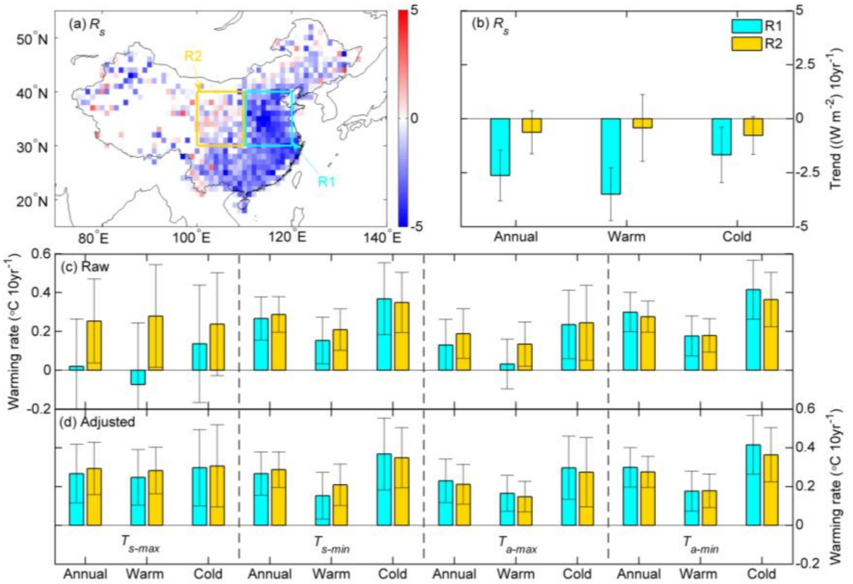

Figure 9. (a) Maps of the trends of surface solar radiation (R_s) and the location of the

regions selected for further analysis: R1 (latitude: 30° –40° N; longitude: 110°–120° W) and R2 (latitude: 30°–40° N; longitude: 100°–110° W). (b) National mean trends for R1 and R2. (c) Annual, warm, and cold seasonal scale trends calculated based on the data before adjustment. (d) Annual, warm, and cold seasonal scale trends calculated based on the adjusted data (Wang et al., 2015a), which did not include the effect of the R_s variations. All error bars indicate the 95% confidence interval.

Table 1. Warming rates (unit: °C 10yr^{-1}) of the temperatures ($T_{s\text{-}max}$, $T_{s\text{-}min}$, $T_{a\text{-}max}$, $T_{a\text{-}min}$) for the annual, warm and cold seasonal scales. Raw and Adjusted represent the warming rates calculated for the data before and after adjusting for the effect of surface solar radiation (R_s) and precipitation (P), respectively. In Method I, the national mean anomalies were calculated first and then the national mean trend based on this time series was calculated. In Method II, the trend of each grid was calculated first and then the national mean value of the trends of all grids was calculated using the area-weight average method. We calculated the national mean trends of the temperatures using both methods.

			$T_{s\text{-}max}$	$T_{s\text{-}min}$	$T_{a\text{-}max}$	$T_{a\text{-}min}$
Method I	Raw	Annual	0.227±0.091	0.315±0.058	0.167±0.068	0.356±0.057
		Warm	0.172±0.103	0.221±0.054	0.091±0.056	0.245±0.049

		Cold	0.354±0.149	0.447±0.101	0.294±0.123	0.505±0.098
	Adjusted	Annual	0.373±0.068	-	0.222±0.062	-
		Warm	0.350±0.064	-	0.160±0.046	-
		Cold	0.450±0.119	-	0.329±0.114	-
Method II	Raw	Annual	0.254±0.197	0.328±0.094	0.183±0.103	0.368±0.082
		Warm	0.193±0.285	0.235±0.095	0.104±0.109	0.256±0.081
		Cold	0.321±0.267	0.415±0.159	0.264±0.167	0.476±0.139
	Adjusted	Annual	0.401±0.137	-	0.239±0.086	-
		Warm	0.374±0.173	-	0.174±0.082	-
		Cold	0.432±0.208	-	0.304±0.152	-

Units: °C $10yr^{-1}$. ±95% Confidence interval.

~~Figs. 13. (a) Maps of the trends of the surface solar radiation (SSR) and the location of the selected regions, R1 (latitude: 30° N–40° N; longitude: 110° N–120° N) and R2 (latitude: 30° N–40° N; longitude: 100° N–110° N). (b) The national mean trends of R1 and R2. (c) The trends on the annual, warm, and cold seasonal scales calculated based on the raw data (Raw). (d) The trends on the annual, warm, and cold seasonal scales calculated based on the adjusted data (Wang et al., 2015a), which does not include the impact of the surface solar radiation variation.~~

~~Table 1. The warming rates (units: °C $10yr^{-1}$) of the temperatures on annual, warm, and cold seasonal scales. Raw and Adjusted represent the warming rates calculated for the data before and after adjusting for the impact of solar radiation and precipitation. Method I represents the first method, which calculates the national mean anomalies first and then calculates the national mean trend based on this time series; Method II represents second method, which calculates the trend of every grids first and then calculates the national mean value of the trends of all grids using the area weight average method. We calculated the national mean trends of the temperatures using both methods.~~